

SIMULATION OF HEAT AND MASS TRANSFER IN ROTARY KILNS

A Thesis Submitted
In Partial Fulfilment of the Requirements
for the Degree of
MASTER OF TECHNOLOGY

By
MOHD. MOZAFFAR JAVED

to the

DEPARTMENT OF CHEMICAL ENGINEERING
INDIAN INSTITUTE OF TECHNOLOGY KANPUR
NOVEMBER, 1979

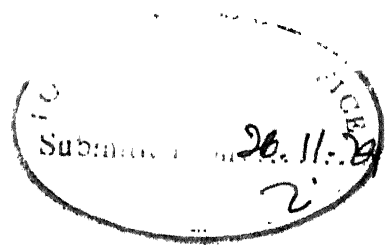
CHE-1979-M-JAY-SIM

I.I.T. KANPUR
CENTRAL LIBRARY

Acc. No. **A 62132**

3 MAY 1980

C E R T I F I C A T E



This is to certify that the work "SIMULATION OF
HEAT AND MASS TRANSFER IN ROTARY KILNS" has been carried
out under our supervision and has not been submitted else-
where for a degree.

A handwritten signature in cursive script, appearing to read "S. Bhatia".

S. Bhatia, Ph.D.
Assistant Professor
Thesis Co-Guide

A handwritten signature in cursive script, appearing to read "H. Veeramani".

H. Veeramani, Ph.D.
Professor
Thesis Supervisor

Department of Chemical Engineering
INDIAN INSTITUTE OF TECHNOLOGY,
KANPUR 208016.

Date : 24th Nov, 79

ACKNOWLEDGEMENTS

I wish to acknowledge with sincere gratitude the valuable advice and encouragement of Professor H. Veeramani who suggested this problem and under whose able guidance the work was carried out.

I am also thankful to Mr. D.S. Panesar for his help in drawing the figures and Mr. B.S. Pandey for his excellent typing.

Finally, I wish to express my thanks to A.C.C. Ltd., Thane, K.C.P. Limited, Madras, West Coast Paper Mills, Karnataka and Central Pulp Mills, Surat for supplying data on their rotary kilns without which this work would not have been possible.

M. Javed
Author

LIST OF FIGURES

FIGURE		Page
2.1	Sketch of a typical rotary kiln . .	6
3.1	Path of a particle in a rotary kiln	16
3.2	Sectional view showing periodic sliding of charge . . .	16
3.3	Geometry of an inclined drum . . .	20
3.4	Partially filled drum section . . .	20
4.1	Heat transfer coefficients in the burning zone as given by Pearce [1] . . .	31
4.2	Flame length and primary air flow as given by Rhuland [37] . . .	31
5.1	Flow chart for simulation program	44
6.1	Temperature and composition profiles for cement kiln (ACC Ltd.) . . .	59
6.2	Temperature and composition profiles for cement kiln (Lyons et al. [41])	60
6.3	Temperature and composition profiles for cement kiln (KCP Ltd.) . . .	61
6.4	Temperature and composition profiles for lime sludge kiln (Labby [40])	62
6.5	Temperature and composition profiles for lime sludge kiln (West Coast Paper Mills) . . .	63
6.6	Influence of cement raw mix moisture on fuel requirement . . .	64
6.7	Influence of lime sludge moisture on fuel requirement . . .	65

LIST OF TABLES

TABLE		Page
1.1	Summary of earlier investigations on rotary kilns ...	4
2.1	Typical rotary kiln installations	12
5.1	Heat transfer coefficient correlations Sass [39] ...	36
5.2	Arrhenius' constants and heats of reaction	38
5.3	Input/Output parameters for simulation program ...	42
6.1	Rotary kiln data supplied by cement/lime manufacturers ...	53
6.2	Simulation of rotary cement kiln (ACC Ltd)	54
6.3	Simulation of cement rotary kiln (Lyons[41])	55
6.4	Simulation of rotary cement kiln (KCP Ltd.)	56
6.5	Simulation of lime sludge kiln (Lobby[40])	57
6.6	Simulation of lime sludge kiln (West Coast Paper Mills) ...	58
A.1	ASTM classification of cements and average composition ...	72
A.2	Reactions in a rotary cement kiln	73

NOMENCLATURE

A	heat transfer area/unit length of kiln
B	clinkerable mass/unit length
b	axial displacement of charge when kiln turns through angle $d\phi$
C	CaO/unit clinkerable mass
C_1	CaO as CaCO_3 /unit clinkerable mass
C'	CO_2 /unit clinkerable mass
C_p	specific heat
D	diameter
D_i	inner diameter
D_o	outer diameter
f	convective term in heat transfer coefficient
F	surface area of kiln charge exposed to gases
G	specific loading of burden material/unit volume of kiln
G'	specific loading of burden material/unit inner surface area of kiln
G_B	clinkerable mass flow rate
G_g	gas mass flow rate
G_N	nitrogen mass flow rate
G_S	burden mass flow rate
H	heat of reaction
h	heat transfer coefficient
k	reaction coefficient
L	length of kiln

M	molecular weight
n	number of revolutions/min
p	partial pressure
q_{CO_2}	heat transmission by radiation for CO_2
$q_{\text{H}_2\text{O}}$	heat transmission by radiation for water
Q	overall heat transmission
Q_{rad}	overall heat transmission by radiation
RF	rate of combustion/unit length of kiln
RW	rate of evaporation of water/unit clinkerable mass
S	thickness of gas stream adjacent to kiln wall
S_1	SiO_2 /unit clinkerable mass
t	time
T	temperature
U_{rad}	overall radiation heat transfer coefficient
V	volume of charge material
W	water/unit clinkerable mass
W'	water/unit N_2 mass
W_M	axial velocity of burden material in rotary kiln
W_{M0}	axial velocity of burden material in rotary kiln when ϕ_M is 0.
X	$(\text{CaO})_2\text{SiO}_2$ /unit clinkerable mass
Y	$(\text{CaO})_3\text{SiO}_2$ /unit clinkerable mass

Greek Symbols

α	modified heat transfer coefficient as defined by eq.(5)
β	static angle of slide for burden material

β^*	dynamic angle of slide for burden material
γ	angle pertaining to geometry of revolving drum defined by eq.(3.3)
ϵ	emissivity factor
ϕ	angle subtended by charge to center of kiln
ϕ_M	volume fraction of kiln occupied by burden material
δ	half central angle subtended by charge to center of kiln
ν	angle of inclination of kiln to horizontal
ρ_M	bulk density of burden material
ω	angular speed of revolution of kiln

Subscripts

1	gas to wall
2	gas to solid
3	inside wall to solid
4	inside wall to outside wall
5	outside wall to ambient
a	ambient
C	convection
g	gas
m/s	charge material
R	radiation
w	inside wall
w'	outside wall

ABSTRACT

This thesis deals with the simulation of transport processes in rotary lime sludge/cement kilns. Using a semi-theoretical approach based on fundamental theory a process model was developed. Sets of equations for chemical reactions, mass flow, and heat flow were solved simultaneously on a digital computer to give profiles of temperatures and compositions as a function of position in the kiln. Effect of reducing water level in the slurry feed was also studied. The results of the simulation agree well with the performance of operating rotary kilns.

CHAPTER 1

INTRODUCTION

Rotary kilns are used in several process applications by virtue of their simple and reliable operation and low maintenance cost. Some typical commercial uses of the rotary kiln are in the manufacture of cement, lime from limestone/dolomite/lime sludge, roasting of ores such as gold, silver, iron etc., production of sodium aluminium sulphate, reduction of iron ore to obtain nodules for blast furnace charge, calcination of sodium bicarbonate, calcination of petroleum coke, etc.

Raw material is fed to the kiln in the form of slurry/ moist solids/pulverised solids and is contacted counter-currently with hot combustion gases obtained from the burning of fuel oil, natural gas or pulverised coal as energy source. The final product is withdrawn as a free flowing solid from the hot end of the kiln and the combustion gases leave from the feed end of the kiln. In general, material is processed through the following zones in the rotary kiln: drying zone, heating zone, reaction zone and soaking zone. The complexity of the heterogeneous solid/ liquid/gas system increases from the feed to the product end with the transformations accompanying the physico-chemical changes as the kiln burden is processed through the various zones of the kiln.

This study deals with the analysis of heat and mass transfer processes accompanied by chemical reactions in rotary kilns. A model is developed for a cement kiln and subsequently applied for the relatively simple lime sludge kiln. Rotary kilns have been the subject of study in several earlier investigations [1,3,5,6,7,21,23,39,40,41],, and the salient features of these studies are summarised in Table 1.1. Some of these studies are empirical in nature [5,6] while others pertain to certain specific zone or aspect of kiln operation/performance [39,41]. A mathematical model is necessary for simulating the performance of a rotary kiln. In this study, a model is developed based on mass and energy balance and supplemented by the findings of various investigations.

Process models for rotary kilns based on a complete theoretical description of the system require specific physico-chemical data. The latter is often not available over the range of conditions of kiln operation. An empirical model based on plant data will be useful for the kiln studied and limited in its applicability to other kilns due to variations in design and operating practices. The process model developed in this study is a semi-theoretical one based on fundamental theory, and includes empirical estimates of unknown parameters. The model can be used for the simulation of operating rotary kilns to assess performance

and to study the influence of changes in major operating parameters as also for process design of rotary kilns. The model is developed based on principal heat transfer mechanisms and the chemical reactions in the various zones. For estimating the residence time of the charge material in the rotary kiln theoretical and semitheoretical models developed by various workers was used [23,21].

The model is used in conjunction with plant data to simulate rotary kiln for production of (i) cement clinker by wet process and (ii) lime by calcination of lime sludge from a pulp mill. The model gave very good agreement (within 8.1 per cent of the fuel consumption) in all the cases.

TABLE 1.1: SUMMARY OF EARLIER INVESTIGATIONS ON ROTARY KILNS

Author	Topics investigated
Sass [39]	Simulation of the drying zone in wet process kilns
Pearce [1]	Model for heat transfer inside the charge in rotary kilns
Zablotny [23], Khodorov [21]	Movement of charge in Rotary Kilns
Imber and Pashkis [3]	Rotary kilns as recuperative heat exchangers
Weber [5]	Temperature and composition measurements in rotary kilns
Folliot [6]	Heat transmission in rotary kilns
Lyons [41]	Chemical reactions in cement kilns
Gygi [7]	Thermodynamics of cement kilns

CHAPTER 2

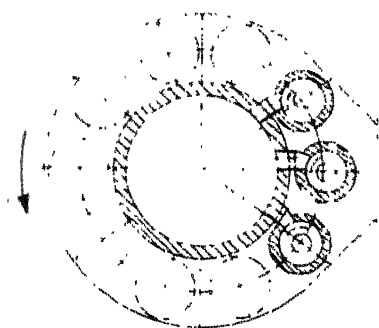
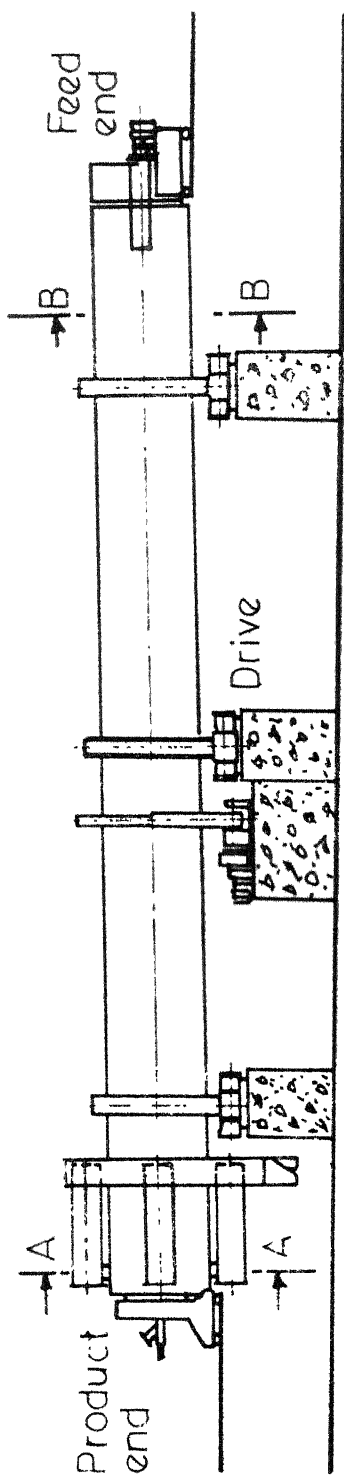
MECHANICAL AND OPERATIONAL ASPECTS OF A ROTARY KILN

2.1 Mechanical Aspects:

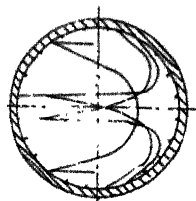
A rotary kiln is essentially an inclined cylindrical steel shell mounted on roller bearings as shown in Figure 2.1. It is lined with refractory bricks to prevent overheating of the steel. Occasionally two linings are used, the one next to the shell being an insulating brick. Insulation on the outside of the shell is generally not used.

The feed is introduced into the upper end of the kiln by various methods, i.e. inclined chutes, overhung screw conveyers and slurry pipes. Sometimes ring dams or chokes of a refractory material are installed within the kiln to build a deeper bed. The hot product is discharged from the lower end of the kiln into quench tanks, onto conveyers, or into cooling devices which may or may not recover the heat. These cooling and heat recovery devices include rotating inclined cylinders, inclined slow moving grates, shaking grates, etc.

Typical sizes of rotary kiln installations are shown in Table 2.1. Some kilns may have two or three diameters to increase kiln capacity, decrease fuel consumption and



A-A
Firing end (with coolers)



B-B
Feed end (with heat exchanger chains)

Fig. 2.1 - Sketch of a typical rotary kiln.

7
improve product quality. Often an enlarged cross-section at the hot end is provided to increase the hold up time at high temperatures.

Modern rotary kiln shells are of all welded construction with riding rings of forged or cast steel and sleeve type main bearings. Power is transmitted to the rotary kiln through gears which are helical or spur with automatic spray lubrication.

Kiln inclination varies with processes from 1° to 4° and peripheral speeds may vary from very slow (0.9 m/min) for a titanium oxide kiln to (38.0 m/min) for a unit calcining phosphate materials.

Accelerated drying of slurries in the feed end of the rotary kiln in wet process operations is achieved by installation of a system of hanging chains, buckets or flights. With the chain system, slurry is heated in three ways: by direct radiation transfer, from chains suspended in hot gases, and by convective transfer due to the flow of the hot gases over the slurry bed. The product is obtained as uniform granules in most applications of the rotary kiln.

The fuel used in the kiln may be either gaseous, liquid, or powdered solids. The burner pipe is installed in a housing consisting of a fixed or movable kiln hood. A center position for the fuel pipe is used when the flame is wanted off the charge. Quite often an off center position for the

fuel pipe is also used. With oil or gas as fuel upto 40 per cent of the stoichiometric air requirement is blown through the burner tube without swirl. A pressure jet oil gun or gas lance passes down the middle of the primary air tube. Coal burners are, in general, of slightly more elaborate design consisting of two or three concentric tubes. In the latter which three tubes, the inner most is for coal transport and the middle and outer tubes are used for primary air. Primary air circulation may be swirled to increase combustion intensity, by directing it through the middle tube fitted with helical vanes.

Other minor mechanical features of rotary kilns include scoop system for recycling collected dust, or in some cases for introducing a feed component through the shell at some intermediate point or points. Dust recovery equipment include cyclones, settling chambers, scrubbing towers and electrical precipitators.

2.2 Operational Aspects of a Rotary Kiln:

From an operational standpoint rotary kilns may be broadly classified as dry process or wet process rotary kilns depending on the moisture content of the feed material. Generally a dry feed kiln will have three zones of heating and a wet kiln will have four:

1. drying ~~zone~~ at feed end for the removal of free moisture.

2. heating zone where the charge is heated to the desired reaction temperature (i.e., the decomposition temperature for limestone or 'burning' temperature for cement).
3. reaction zone in which the charge is burned, decomposed, reduced, oxidised, etc.
4. Soaking zone where the reacted charge is superheated or 'soaked' at temperature or, if desired cooled before discharge.

The heat transfer mechanisms in the various zones of the kiln are obviously not the same. In the first two zones the dominant heat transfer mechanism is convection from the hot kiln gases to the burden material (Partly through the intermediary wall or hanging chains). In the last two zones the dominant heat transfer mechanism is radiation from the hot gases and the flame.

As the charge material proceeds from one zone to another its physical and chemical properties undergo changes. For example, in the wet process cement rotary kiln the feed slurry (35 per cent moisture) is thick and does not flow freely. Chains in the drying zone serve as surfaces upon which the material can accumulate until it is not longer sticky at which time it will break off as a granular solid and continue its movement into the heating zone. At the beginning of the reaction zone, temperatures are high enough (800-900°C) to cause a decomposition of the calcium carbonate.

However, it is not before the clinkering reactions that the charge starts to melt. In practice, there are no sharp dividing lines between the various zones. Bogue [25] considers that reactions giving cement compounds can start as early as 600°C which would normally be considered to fall in the heating zone.

The attainable thermal efficiency in the burning of clinker in modern rotary kilns is about 50 per cent. Roughly 20 per cent of the heat is lost by radiation through the walls and about 30 per cent with the gas going to the stack. A small amount of heat is lost in the solids coming out of the recuperative heat exchanger. The heat recovered in the coolers is used to preheat the combustion air to the rotary kiln. With the present day internal heat exchangers the exit temperature of the gas is about 50°C above the dewpoint of the gas. It is generally not advisable to recover heat any further from the flue gases in order to prevent corrosion problems in the auxiliary dust collection equipment installed before the stack.

Cyclones or electric precipitators installed with rotary kilns are very efficient for the collection of entrained dust from the stack gas. In the rotary kiln fine particles of charge material are carried along the form of dust by the combustion gases. The quantity of dust increases with the gas velocity, the proportion of fine particles in the material

and with the number of heat exchanger inserts. For the majority of the wet process cement rotary kilns the dust quantity is between 2 and 5 per cent as referred to the clinker throughput. Part of the dust produced in the rotary kiln is precipitated in the drying zone and is carried along by the charge material back towards the kiln outlet. In this way an 'internal dust cycle', or internal circulation of dust is brought about. The dust which is not precipitated in the kiln itself is for the most part collected in the electrostatic dust collection plant and returned directly to the kiln inlet. In this way an 'external dust recycle' is established.

TABLE 2.1: TYPICAL ROTARY KILN INSTALLATIONS

Size Diam. x Length (m x m)	Portland cement (tpd)		Lime (tpd)	
	Dry Process	Wet Process	Lime sludge	Lime stone
1.52 x 24.38	23.5	16.8	10.0	16.0
1.82 x 21.33	31.9	22.6	15.0	24.0
2.13 x 21.33	46.2	33.6	20.0	35.0
1.68 x 54.86	47.8	41.9	30.0	45.0
2.13 x 36.57	79.7	57.1	35.0	55.0
2.28 x 38.10	96.5	69.7	40.0	70.0
1.82 x 67.05	70.5	63.0	45.0	65.0
2.43 x 42.66	125.9	90.6	55.0	90.0
2.74 x 48.76	184.6	134.0	80.0	130.0
2.43 x 91.43	193.0	167.9	110.0	160.0
3.20 x 56.38	302.0	218.2	130.0	190.0
3.20 x 76.20	293.8	256.0	175.0	240.0
3.35 x 91.43	402.9	352.5	225.0	300.0
3.50 x 91.43	436.4	377.6	240.0	320.0
3.50 x 144.77	671.4	587.5	375.0	450.0
3.66 x 152.39	772.1	671.4	425.0	500.0

CHAPTER 3

The rotary kiln is a countercurrent reactor in which mechanical, thermal and physico-chemical changes are taking place simultaneously, and it is necessary to know the residence time of the material in the various sections for a rational design of the system. The hold up of the material in individual zones of the kiln is a function of the rate of shifting of the material along the kiln axis. This rate depends on many factors, such as the inclination of the kiln, diameter, the number of revolutions per minute, the rheological properties of the charge material and the presence of internal structural obstructions in the kiln. In a wet process rotary kiln the change in physical properties of the burden material from the feed to product end is quite substantial. The somewhat sticky slurry at the feed end is converted to a free flowing material after it has passed through the drying section. In the decarbonating zone the solid charge material becomes powdery and flaky after losing carbon dioxide. This leads to an increase in the bulk density of the material. And finally in the reaction and clinkering zones where the temperatures are between 1300-1500°C a degree of melting (20-30 per cent of the charge) occurs sufficient to cause the material to cohere into small balls or lumps of clinker. The charge takes about 2.5 hrs.

to pass through a kiln 60 m long and the time during which it is at the clinkering temperature is, at most, 20 minutes. In view of the fact that the clinkering zone is a small fraction (10-20 per cent) of the overall kiln length it is possible to consider the burden material to be a free flowing solid for studying the material movement in the kiln. Therefore to illustrate the character of the motion we examine a simple example of the motion of free flowing materials in an unobstructed kiln and assume no change in the physico-chemical properties of the materials during their residence in the rotary kiln.

3.1 Mechanism of Motion of the Charge:

During the movement of a rotating cylinder, partially filled with free flowing material, two components appear: the motion of particles of the charge material in the cross-section of the cylinder and the motion along the axis of the cylinder. Sullivan [4], Saeman [17], Boguslavskii [18] and Ronco [19] have described the motion of particles in rotating cylinders. An important factor contributing to the axial movement of the charge is the angle of inclination of the axis of the rotating cylinder to the horizontal and must be greater than the angle of slide of the material for uniform movement. Modern rotary kilns have an inclination of 3-5 per cent and being considerably less than the angle of slide of the materials a uniform shifting of the entire mass does not occur. In these

units the charge consists of a layer 1-5 cm thick and is lifted by the wall in the direction of rotation of the cylinder. As a result of this, the angle of inclination of the surface of the charge is close to the angle of slide for the material. The angle of slide of charge materials usually lies between 20° - 40° . In industrial processes the layer of charge usually occupies 8-20 per cent of the volume of the kiln.

To explain the motion of the charge in rotary kilns, the above authors examined the motion of individual particles of the material. In any cross-section, a particle of material present in the charge cannot be shifted along the kiln at a rate different from the velocity of all particles of the material surrounding it. During rotations of the kiln, individual particles of free flowing material are shifted along the axis of the kiln in a flattened helical motion. Diomidovskii [46] described the motion of particles in a rotary kiln in the following manner: a particle of material located in the bottom layer of the charge at point 1 (Fig.3.1), during rotations of the cylinder moves together with the charge along the path (arc 1-1'), then, by the effect of gravity that particle rolls from point 1' along the slanting surface to point 2, from which it again travels with the charge along the path (arc 2-2') and emerges on the surface at point 2'. This pattern of particle movement is also

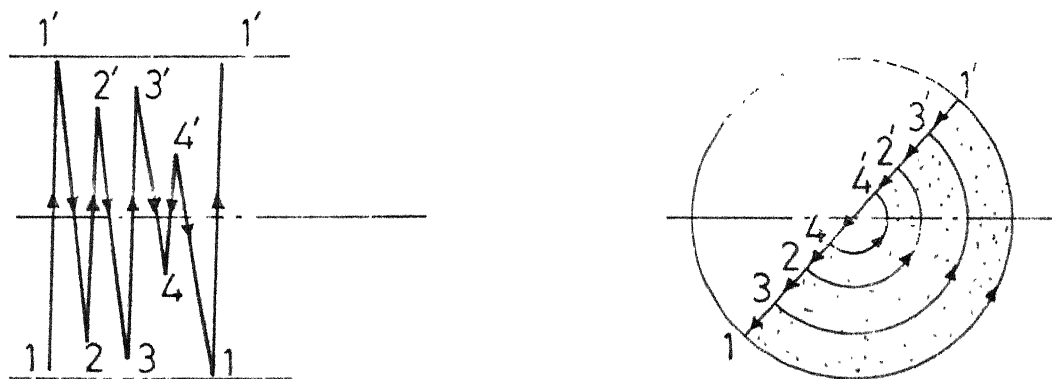


Fig.3.1 - Path of a particle in a rotary kiln.

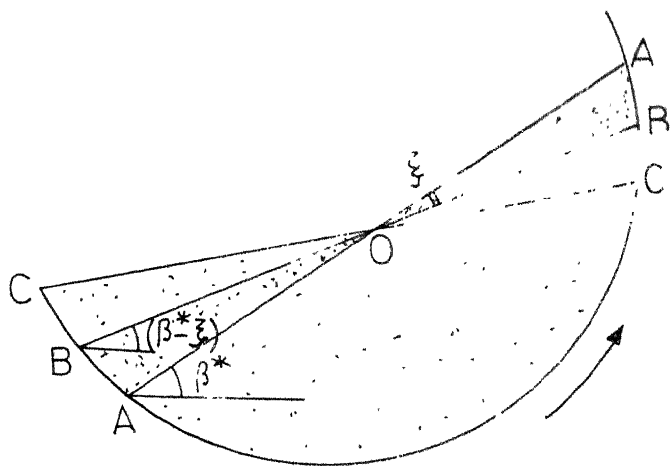


Fig. 3.2 - Sectional view showing periodic sliding of charge.

illustrated by 3-3' and 4-4' in Figure 3.1. The forward progressive motion occurs only when the path of the rolling of the particles over the surface of the material forms an (internal) angle of less than 90° with the axis of the kiln.

The material slides periodically, in the manner of an avalanche, from the top to the bottom part of the charge on the surface (Fig.3.2). When the surface of the charge is level or forms with the horizontal plane an angle smaller than the angle of slide of the material, rolling of the particles on the surface cannot occur. This situation is shown in Figure 3.2. by the straight line C-C. During the rotary motion of the cylinder, the surface of the charge gradually moves from position C-C into the position A-A, forming the angle β with the horizontal. At the moment the surface of the charge attains position A-A, the surface layer of the charge is detached in the upper part of the segment and then sliding of the material begins. The quantity sliding down is shown schematically in Figure 3.2 by the line AOB, which simultaneously forms the angle ξ , called the shearing angle. After rapid sliding of that part of the material, the surface of the charge is in dynamic equilibrium, as it rests at an angle smaller than the angle of slide by the shearing angle. The next portion of the material can slide on the surface of the charge only when that surface as a result of rotation of the cylinder again is on the straight line AA. Therefore, the

motion of particles is subject to periodic sliding of the surface layer.

Diomidovskii [46] states that the shearing angle has been determined experimentally and that it depends on the physical properties of the charge material as well as the number of revolutions per minute of the cylinder. At 1-2 rpm the shearing angle for cement is $12-15^{\circ}$. When the speed is increased to 4-6 rpm, however, the shearing angle diminishes rapidly to zero. Some confirmation of this is given by Boguslavskii [18] for rotary soda calciners (4 rpm), who observed the sliding of only a thin layer of material, and the theoretical thickness of this layer was equal to the linear size of the particles (the diameter). Moreover, he concluded that particle size has no influence on the output of the kiln or the flow rate of charge, as the diameter of the particles had no influence on the angle of slide of the material. Therefore, the formulae for calculation of the rate of shifting will not include the particle size of the material. If this condition is not fulfilled, then during rotations of the kiln the charge will be elevated only to a height at which the angle between the surface of the material and the horizontal is less than the angle of slide. Then the particles will not roll on the surface of the charge and only sliding of the entire section of the charge along the walls of the kiln will occur.

3.2 Rate of Charge Movement:

In this section a mathematical derivation of the axial velocity of the material in a rotary kiln is outlined. The rate of charge shifting depends on the production rate, diameter, speed and volume fraction of the kiln occupied by the charge.

Figure 3.3 shows the geometry of an inclined rotating cylinder. From this figure one can obtain for the geometry of the flow of charge material:

$$\sin \gamma = \frac{\sin \psi}{\sin \beta} \quad (3.1)$$

$$\tan \gamma = \frac{\sin \psi}{\sin \beta^*} \quad (3.2)$$

$$\text{and } \sin \beta^* = \sin \beta \cos \gamma \quad (3.3)$$

where

β = angle of slope (static angle of slide)

β^* = apparent angle of slope (dynamic angle of slide)

ψ = angle of inclination of drum

(a) Transport of material if the volume fraction of kiln occupied by material is zero.

$$\Delta L = \pi D \tan \gamma \quad (3.4)$$

$$\Delta t = \frac{60}{n} \quad \text{where } n = \text{rpm of kiln} \quad (3.5)$$

$$W_{MO} = \frac{\Delta L}{\Delta t} = \text{Axial velocity when volume fraction } \phi_M \text{ is zero} \quad (3.6)$$

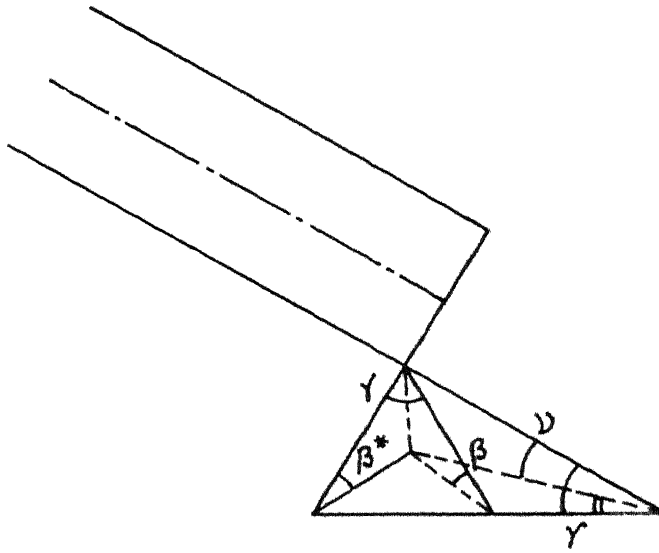


Fig. 3.3 - Geometry of an inclined drum.

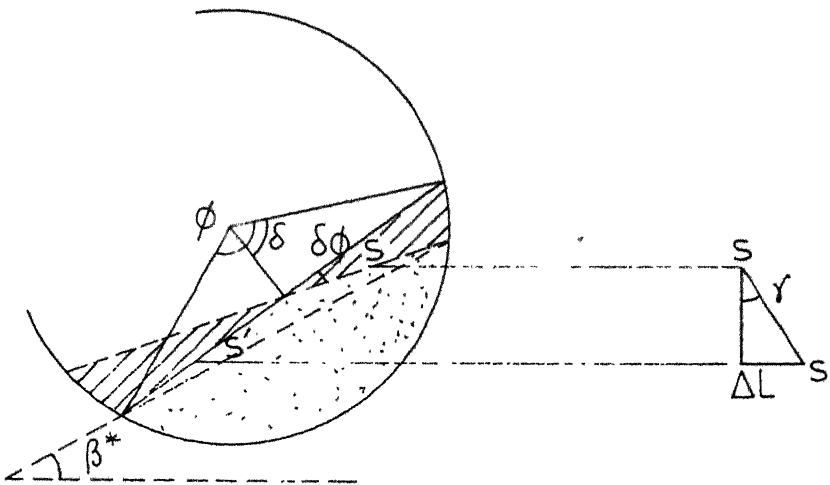


Fig. 3.4 - Partially filled drum section.

$$W_{MO} = \frac{D n \pi \tan \gamma}{60} \quad (3.7)$$

(b) Transport of material if the volume fraction of kiln occupied by material is finite and equal to ϕ_M .

At a partly filled drum section the transport of material is caused by gliding of the highest layer as shown in Fig. 3.4. Turning through the angle $d\phi$ we get for the hatched volume of material

$$dV = R \sin \delta \cdot R d\phi \sin \delta b$$

where b is the forward displacement

A displacement of the centre of gravity from S to S' gives

$$\Delta L = \frac{1}{3} D \sin \delta \tan \gamma \quad (3.8)$$

$$V = \frac{\pi}{4} D^2 \phi_M b \quad (3.9)$$

Therefore the centre of gravity is displaced by

$$\Delta L = \frac{dV}{V} \text{ in the time } dt = \frac{d\phi}{\omega}; \quad \omega = 2\pi n/60.$$

The axial velocity of the material may then be expressed as

$$W_M = \frac{\Delta L}{V} \frac{dV}{dt} = \frac{D \cdot n \cdot \sin^3 \delta}{90 \phi_M} \tan \gamma \quad (3.10)$$

$$W_M = \frac{D \cdot n \cdot \sin^3 \delta \sin \gamma}{\sin \beta \cdot 90 \left(\frac{\delta}{\pi} - \frac{\sin 2\delta}{2} \right)} \quad (3.11)$$

For $\delta=0$, i.e. when the filling is zero, W_{MO} goes to 0/0 and leads to the following term after differentiating the numerator and denominator with respect to δ

$$W_{MO} = \frac{D \cdot n \cdot \pi \cdot \tan \gamma}{60} \quad (3.12)$$

$$\frac{W_M}{W_{MO}} = \frac{2 \sin^3 \delta}{3(\delta - \frac{1}{2} \sin 2\delta)} \quad (3.13)$$

The material transported per hour is represented by equation(3.14)

$$G_M = \frac{\pi}{4} D^2 \rho_M \cdot W_M \cdot 3600 \rho_M \quad (3.14)$$

ρ_M = bulk density of material

A number of formulae similar to 3.11 have appeared in the technical literature [4,17,22,20,21,23]. These formulae which are derived on the basis of theoretical premises or statistical analysis attempt to give the linear velocity or the rate of shifting of the charge in a rotary kiln. Some of these are listed below:

Sullivan [4]

$$W_M = 0.565 D \cdot n \cdot \frac{\nu}{\beta^{1/2}} \quad (3.15)$$

Saeman [17]

$$W_M = \frac{3.14 D \cdot n \cdot \nu}{\sin \beta} \quad (3.16)$$

Bayard [22]

$$W_M = 3.24 \frac{D \cdot n \cdot \nu}{(24 + \beta)} \quad (3.17)$$

Baranowskiif [20]

$$W_M = 2.32 \frac{D \cdot n \cdot \nu}{\sin \beta^*} \cdot \frac{\sin^3 \delta}{(2\delta - \sin 2\delta)} \quad (3.18)$$

Khodorov [21]

$$W_M = \left[1 + 0.00257 \cdot \frac{120 \delta}{n} \sqrt{\frac{g(\sin \beta^* - \tan \beta \cos \beta^*)}{D \sin \delta}} \frac{\pi}{45} D \right] \quad (3.19)$$

Zablotny [23]

$$W_M = 0.735 \pi D n \left(\frac{\lambda}{\beta} \right)^{0.85} \quad (3.20)$$

Zablotny's [23] correlation is used in the present work in equation 5.6. The latter correlation derived on a semi-theoretical and statistical basis is superior to the others [4,17,22] which are derived from theoretical considerations. Khodorov [21] and Baranowski's [20] correlations are more involved.

CHAPTER 4

HEAT TRANSFER IN ROTARY KILNS

4.1 Heat Transfer Mechanism:

Gygi [8] studied heat transfer in a wet process rotary kiln for cement manufacturing in 1937 and his work still forms the basis for several present investigations.

The transmission of heat along the axis was calculated on the basis of the experimental data. The calculations showed that heat transfer in the hot zones of the kiln was mainly by radiation, in which the free exposed wall of the kiln acted as indirect heating surfaces. In the cooler parts of the kiln, however, heat transmission by radiation diminishes, and transmission by convection is more important. In the above heat transfer calculations the influence of the dust content of the gases was ignored by Gygi.

Folliot [6] calculated the transmission of heat in the preheating, drying, calcining and sintering zones of an experimental rotary kiln ($D_F = 2.78$ m, $L=45$ m) by measuring the temperature of the gases, kiln wall, and material in the kiln. It was observed that the amount of heat transfer to the material as given by Gygi was larger than the amount actually transmitted. Folliot has attributed this to an erroneous calculation of the emissivity factor of the gas by Gygi.

In the preheating, calcining and sintering zones about 84 per cent of the heat supplied to the kiln charge is transmitted by radiation and convection from the gas and by radiation from the wall (90 per cent of this heat is transmitted by radiation and 10 per cent by convection). The balance of the heat transfer (16 per cent) is supplied to the material by the 'wall effect' (convection effect of the refractory), this being the heat that is stored up in the lining and is transferred to the material at each revolution of the kiln. The wall effect increases only slightly with the thermal conductivity of the lining, but it increases considerably with the thermal conductivity of the charge material.

Owing to the loose packing of the charge material in a rotary kiln it acts as a good heat insulator: the energy transmitted to the surface is not entirely carried away to the interior of the layer of material and the result is that a thin surface layer becomes highly heated. The radiation emissivity of the layer of material is less than unity, and therefore part of the heat absorbed is reflected. The reflectivity coefficient (reflected heat/total heat absorbed by radiation) increases with higher material temperature and greater fineness of grain for grain sizes above 1 mm it ceases to change however. Folliot [6] gives the following values for this reflectivity coefficient: raw meal 0.20; decarbonated raw meal 0.30; and clinker 0.20.

Most investigators have taken the burden to be well mixed and consequently assumed that the outer layer of the burden has the same temperature as the interior of the burden. Wachters and Kramers [33] have studied heat transfer to granular material in a rotating cylinder. An experimental model ($D = 0.152$ m, $L = 0.475$ m) with a heated wall was used with dry sand as the kiln material. They have observed that the solid mixing process have a significant effect on the overall heat transfer rates. However, equations developed by Wachters and Kramers are not applicable to the direct fired rotary kilns. Pearce [1] in his study attempted to derive a solid state side heat transfer coefficient. Pearce pointed out that the gas cannot radiate heat to a particle situated within the charge material. It can do so only if the particle rises to the surface. Its retention time at the surface will depend on the circulatory motion within the material. In course of this movement the particle heats up very rapidly and acquires a far higher temperature than the general mass of the material. It then disappears into the mass, where it gives up the heat that it has absorbed so that the heating of the mass of the material is accomplished by a sort of 'solid convection'!

The transmission of heat from the flame to the material is therefore effected in two stages:

(a) Heating of a thin layer of the material by radiation and convection from the gas and by radiation and conduction from the kiln wall.

(b) Transmission of heat accumulated in the layer to the rest of the material.

Measurements by Folliot [6] have shown that for a constant average temperature of 680°C in the mass of the material the surface undergoes a rise of 80°C and 270°C in 0.1 and 1 second respectively, but at a depth of 1 mm below the surface the amount of heat supplied to the material is only one-hundreth of the heat radiated on to the surface. According to Folliot the surface is renewed in less than one second.

4.2 Overall Heat Temperature Coefficients:

From Folliot's investigations and the heat transfer formulae given by Schack [34] and Heliginstaedt [35] it appears that at gas temperatures above $800-900^{\circ}\text{C}$ such as occurs in the preheating, calcining and sintering zones of the wet process rotary kilns and at low gas velocities heat is transmitted almost entirely by radiation. Heat transmission by radiation can be affected only by the carbon-dioxide, water and dust content of the gases. According to Schack [34] equations (4.1) and (4.2) represent heat transmissions by radiation for carbon dioxide and water respectively:

$$q_{\text{CO}_2} = 8.9 (\text{P.S.})^{0.4} \left(\frac{T}{100}\right)^{3.2} \text{ K.cals/hr m}^2 \quad (4.1)$$

$$q_{\text{H}_2\text{O}} = (40-73 \text{ P.S.}) (\text{P.S.})^{0.6} \left(\frac{T}{100}\right)^{2.32 + 1.37 (\text{P.S.})^{1/3}} \text{ K.Cals/hr.m}^2 \quad (4.2)$$

where

P = partial pressure of CO_2 or H_2O

S = thickness of the gas stream

Equations (4.1) and (4.2) show that the transmission of heat by radiation increases with the thickness of the gas stream. The latter is determined by the effective diameter of the kiln: its inner diameter must be multiplied by 0.9 to obtain the thickness of the gas stream [36].

Equations (4.1) and (4.2) show that radiation is approximately proportional to $D^{0.5}$. The exponent may in fact range from 0.4 to 0.6 depending on the constituents of the gas and its dust content. From Folliot's empirical observations the transmission of heat for equal temperature differences between gas and charge is approximately proportional to $D^{0.5}$.

$$Q = 115,000 D^{0.5} \text{ K.cals/hr m}^2 \quad (4.3)$$

The surface area of the kiln charge is obtained for equal grain size, from the loading factor ϕ_M , the length and diameter of the kiln:

$$F = D.L.\sin \delta \quad (4.4)$$

where, D = diameter of kiln; L = length of kiln;
 δ = half of the central angle subtended by the charge
to the centre of the kiln;

$$Q_{\text{rad}} = U_{\text{rad}} \cdot \Delta T D L \sin \delta \quad (4.5)$$

U_{rad} = overall radiation heat transfer coefficient

In view of the foregoing conclusions, one may adopt for the heat transfer coefficient:

$$U_{\text{rad}} = K_o D^{0.5} \quad (4.6)$$

$$Q_{\text{rad}} = K_o D^{0.5} \Delta T D L \sin \delta \quad (4.7)$$

$$Q_{\text{rad}} = K_o D^{1.5} \Delta T L \sin \delta \quad (4.8)$$

K_o = constant

Since 90 per cent of the heat supplied to the charge is in the preheating, calcining and sintering zones of the wet process rotary kilns, the heat transfer in the kiln and consequently also the throughput are for equal temperatures, approximately proportional to the transmission of heat by radiation

$$Q = K_o D^{1.5} L \Delta T \quad (4.9)$$

In equation (4.9), $\sin \delta$ has been dropped because the loading factor in ϕ_M in most modern day rotary kilns is constant between 8-20 per cent and even a 100 per cent variation in ϕ_M causes the value of $\sin \delta$ to change by about 16 per cent only.

In terms of the above considerations the specific throughput can be represented by equations (4.10) and (4.11) for G and G' .

$$G = \frac{K_o D^{1.5} L}{\frac{\pi D^2}{4} \cdot L} = \frac{K_o}{D^{0.5}} t / 24 \text{ hr. m}^3 \quad (4.10)$$

$$G' = \frac{K \cdot D \cdot 1.5 \cdot H}{\pi D L} = K_1 D^{0.5} t / 24 \text{ hr m}^2 \quad (4.11)$$

where K and K_1 are constants ($K = \frac{4}{\pi} K_1$)

G = specific loading per unit volume

G' = specific loading per unit inner surface area.

By a statistical examination of 24 Kilns in actual operation VDZ (Association of German Cement Works) has reported an average value of K_1 of 3.13 (standard deviation 3.7 per cent). The statistical investigators bear out the theoretical considerations as to the transmission of heat in the direct fired rotary kilns. It must be borne in mind, however, that the transmission of heat is also dependent on:

1. The temperature difference between the gas and the material.
2. The dust content of the gases.
3. The loading factor of the kiln.
4. The kiln charge material: particle size, colour etc.

But these four conditions are more or less uniform for similar kilns.

Pearce [1] has given theoretical estimates of heat transfer from a rotary kiln flame. This is shown in Figure 4.1, and it is evident that convective heat transfer also plays an important part in the burning zone. Also included in Figure 4.1 is an estimate of the effect of swirling of the primary air jet and thus leads to a reduction in convective

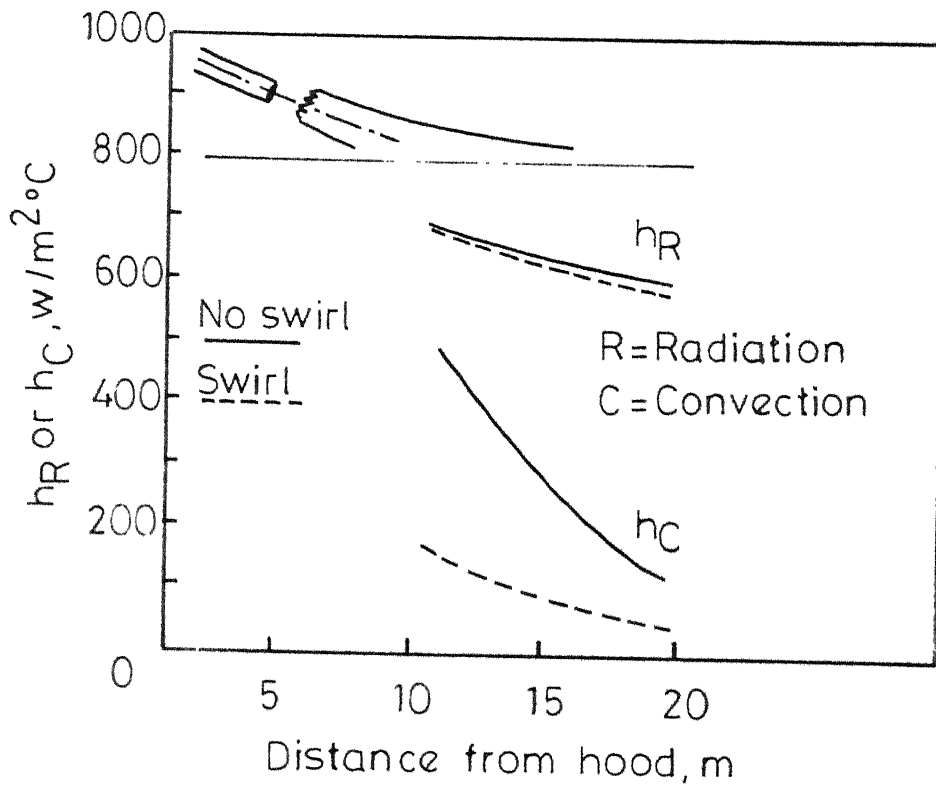


Fig. 4.1 - Heat transfer coefficients in the burning zone as given by Pearce [1].

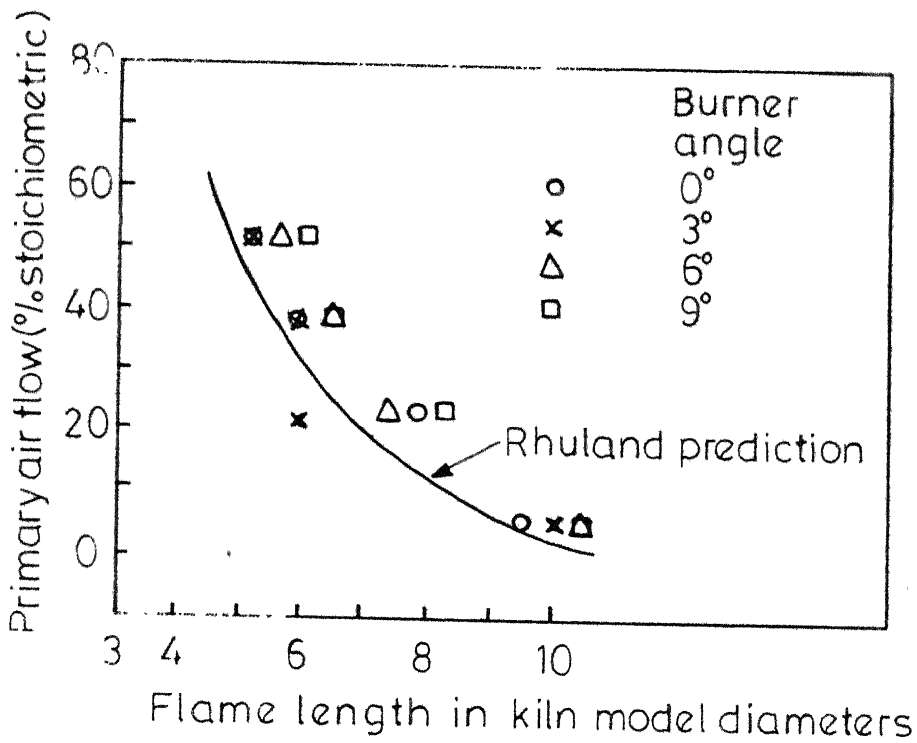


Fig. 4.2 - Flame length and primary air flow as given by Rhuland [37].

heat transfer caused by a decrease in the axial velocity of the flame.

4.3 Estimates of Flame Lengths:

The effect of primary air momentum on flame length and combustion intensity has been studied extensively by Ruhland [37] with both model experiments and plant trials. In his model experiments Rhuland simulated the mixing and combustion processes by reacting dilute acid and alkali solutions with phenolphthalein as indicators in long plastic tubes. The acid solutions being pushed in through a small narrow glass tube placed at the centre of the larger tube containing alkali very much in the same manner as pulverised coal is fed to the rotary kiln through a central fuel pipe. A pink coloured zone was produced which had the essential appearance and characteristics of a flame. Rhuland thus deduced a general equation for flame lengths. At relatively low nozzle velocities Rhuland's equation predicts experimental observations with acceptable accuracy as shown in Figure 4.2. The angle between the kiln and the burner axis has little effect on the flame length.

CHAPTER 5

MODEL FOR TRANSPORT PROCESSES IN ROTARY KILNS

The transport processes occurring in a rotary kiln consist of simultaneous heat and mass transfer with chemical reactions. Each particle in the charge travels in a complex spiral like motion as described in Chapter 3. During a part of its journey through the kiln it remains on the surface of the charge where heat is transferred to it directly by radiation and convection from the hot gases. But most of the time it receives heat indirectly from the other particles when the charge is thoroughly mixed during rotation of the kiln. The complexity of the transport processes in the kiln is further increased by the evaporation of the slurry water, decarbonation of the charge and finally by the liquid formation during clinkering. Solid-solid reactions between the various constituents of the charge (like CaO and SiO_2) and between the intermediates (like C_5A_3 , C_5A and C_3A) are very difficult to analyse. Rate equations for such solid-solid reactions are not known because of their dependence on properties like fineness and homogeneity of the charge material which are difficult to characterize.

However, with certain simplifying assumptions a model may be developed to take into account both heat and mass transfer processes.

5.1 Assumptions

The following assumptions are made:

- (i) All transport processes occur at steady state.
- (ii) Specific heat coefficients, latent heats and heats of reaction are constant at their average values.
- (iii) Convective heat transfer coefficients are independent of temperature.
- (iv) Burden material travels at a uniform velocity through the kiln. The linear velocity of the charge in the kiln is given by equation 3.20.
- (v) Gas wall and solid emissivities are constant at their average values. These values are taken from Lyons [41] for cement kilns and from Libby [40] for lime sludge kilns.
- (vi) No loss of material in the form of dust.
- (vii) Presence of possible impurities and inert compounds are not included excepting in so far as they affect the kinetic factors.
- (viii) Combustion is assumed to be complete.
- (ix) Complete mixing of the burden material during the slumping of the charge after every revolution of the kiln.

Heat transfer occurs in rotary kilns according to the following modes, similar to the study by Sass [39].

- (i) gas to solid by convection and radiation
- (ii) gas to inner wall by convection and radiation
- (iii) inner kiln wall to solid by conduction, and
by radiation from the uncovered portion of the
wall.
- (iv) radial conduction through the kiln wall and
insulation.
- (v) heat losses from the outer wall to ambient air
by radiation and convection .

Heat transfer rates for the above modes can be represented by equation

$$\alpha_i = h_i A_i$$

where h_i = heat transfer coefficient

A_i = heat transfer surface per unit length of kiln

The relationships used for the different modes of heat transfer are summarised in Table 5.1.

Having developed the heat transfer correlations we write down the sequence of reactions occurring in a rotary cement kiln.

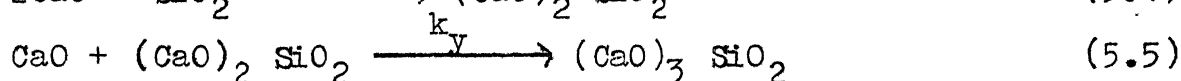
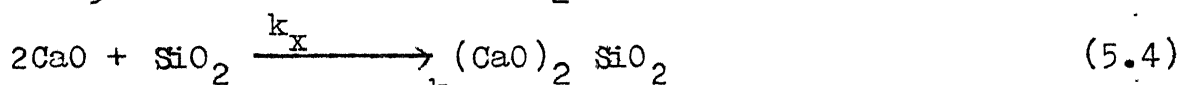
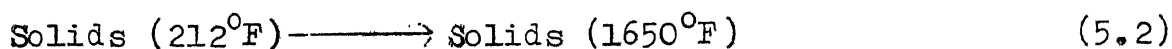
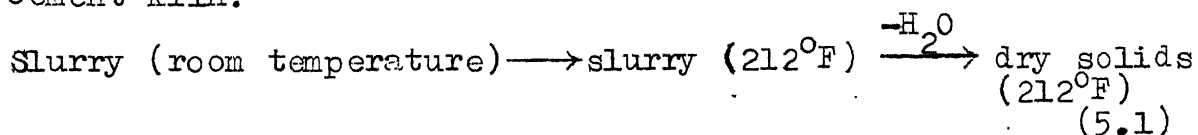


TABLE 5.1: HEAT TRANSFER COEFFICIENT CORRELATIONS. SASS [39]

Heat transfer path	h_i	A_i
Gas to inner kiln wall	$h_1 = f_1 + 0.173 \times 10^{-8} \epsilon_g \epsilon_w (T_g - T_w^4) / (T_g - T_w)$	$A_1 = \pi (1 - \frac{\phi}{360}) D_i$
Gas to solid	$h_2 = f_2 + 0.173 \times 10^{-8} \epsilon_g \epsilon_n (T_g - T_m^4) / (T_g - T_m)$	$A_2 = D_i \sin \phi / 2$
Inner kiln wall to solid	$h_3 = f_3 + 0.173 \times 10^{-8} (\frac{A_2}{A_3}) (\epsilon_w \epsilon_m) \frac{(T_w^4 - T_m^4)}{(T_w - T_m)}$	$A_3 = \pi D_i (\frac{\phi}{360}) + D_i \sin \frac{\phi}{2}$
Inner kiln wall to outer	$h_4 = 2 k_w / (D_o - D_i)$	$A_4 = \pi (D_o - D_i) / \ln (D_o / D_i)$
Outer wall to ambient	$h_5 = f_5 + 0.173 \times 10^{-8} \epsilon_w' (T_w^4 - T_a^4) / (T_w - T_a)$	$A_5 = \pi D_o$

Convective heat transfer coefficients Lyons[41]		
Convective term f , Btu/hr ft ² °F	General	Chain section
f_1 gas to wall	5.01	10.02
f_2 gas to solid	4.02	97.21
f_3 inside wall to solid	39.12	44.13
f_5 outside wall to ambient	5.00	5.00

For the lime sludge kiln we have only the reactions corresponding to equations (5.1) to (5.3). The rate expressions for each of the reactions can be written in the form of the Arrhenius' equation. Table 5.2 gives the Arrhenius' constants and the heats of reaction for the chemical reactions occurring in a rotary cement kiln.

5.2 Temperature and Composition Profiles:

For the purpose of development of differential equations which describe the temperature and composition profiles in the kiln one can divide the kiln into four sections. In the drying zone, the wet solid is heated to the boiling point of the water by the hot gas. It is assumed that no vaporization occurs in this region. In the second region, liquid is evaporated at constant solid temperature. It is assumed that gas temperatures in this region are high enough that the rate of liquid evaporation is not mass transfer controlled. In the third region the charge is raised to calcination/sintering temperature and the equations are identical to those used in the first section except that the values of specific heats and mass flow rates now refer to the dry solid and gas streams. In the fourth region calcination and the cement forming reactions start so that the equations describing the temperature of the material contain the heats of reaction term in addition to the heat transfer terms.

TABLE 5.2: ARRHENIUS' CONSTANTS AND HEATS OF REACTION

Rate constant $k(\text{hr}^{-1})$	Activation Energy, Btu/lb.	Reaction	Heat of reaction, Btu/lb.
7.08×10^7	18,071	$\text{H}_2\text{O}(\text{l}) \xrightarrow{k_w} \text{H}_2\text{O}(\text{g})$	$\Delta H_w = 970$
1.393×10^{27}	261,046	$\text{CaCO}_3 \xrightarrow{k_c} \text{CO}_2 + \text{CaO}$	$\Delta H_c = 1275/\text{lb. CaO}$
5.245×10^{22}	82,644	$2\text{CaO} + \text{SiO}_2 \xrightarrow{k_x} (\text{CaO})_2\text{SiO}_2$	$\Delta H_x = 381/\text{lb. CaO}$
2.78×10^{22}	110,192	$\text{CaO} + (\text{CaO})_2\text{SiO}_2 \xrightarrow{k_y} (\text{CaO})_3\text{SiO}_2$	$\Delta H_y = 0/\text{lb. CaO}$

Using assumption (iii) one may write down the uniform

burden velocity through all the zones as

$$\frac{dL}{dt} = \frac{G_B}{B} = W_M \quad (5.6)$$

In addition the mass flow rate of the burden material and the gas at any section of the kiln are given by equations (5.7) and (5.8) respectively.

$$G_S = G_B \left[1 + \left(\frac{M}{M_C} \right) C_1 + W \right] \quad (5.7)$$

$$G_g = G_N [1 + W' + C'] \quad (5.8)$$

For the first section where the water in the slurry is brought to its boiling point the temperature of the material and the gas are described by the equations (5.9) and (5.10).

$$\frac{dT_m}{dL} = \frac{1}{C_{pm} G_S} [\alpha_2 (T_g - T_m) + \alpha_3 (T_w - T_m)] \quad (5.9)$$

$$-\frac{dT_g}{dL} = \frac{1}{C_{Pg} G_g} [\alpha_2 (T_m - T_g) + \alpha_1 (T_w - T_g) + C_{Pm} (T_m - T_g) \frac{dG_S}{dL} + RF] \quad (5.10)$$

For the second region where the evaporation of water occurs the temperature of the material remains constant. This situation is described by equations (5.11) to (5.13)

$$T_m = \text{constant} \quad (5.11)$$

$$RW = [\alpha_2 (T_g - T_m) + \alpha_3 (T_w - T_m)] / (B \Delta H_w) \quad (5.12)$$

$$\frac{dW}{dL} = - \frac{(RW)B}{G_B} \quad (5.13)$$

The equation for the gas temperature is the same as equation (5.10).

In the third region equations are identical to those used in the first region except that the values C_{Pm} , C_{Pg} , G_g now refer to dry solids and gas streams.

Equations (5.14) to (5.18) are applicable in the fourth zone in which the major reactions occur. The decomposition of calcium carbonate is given by equation (5.14).

$$\frac{dC_1}{dL} = - \frac{k_C C_1 B}{G_B} \quad (5.14)$$

Equations (5.15) and (5.16) are valid for the formation of the cement compounds C_2S and C_3S respectively.

$$\frac{dX}{dL} = \left[\left(\frac{M_X}{2M_C} \right) k_X C^2S - \left(\frac{M_X}{M_C} \right) k_Y CX \right] \frac{B}{G_B} \quad (5.15)$$

$$\frac{dY}{dL} = \left(\frac{M_Y}{M_C} \right) k_Y CX \frac{B}{G_B} \quad (5.16)$$

The disappearance of silica and the formation of free lime follow equations (5.17) and (5.18).

$$\frac{dS_1}{dL} = \left(\frac{M_{S_1}}{2M_C} \right) k_X C^2S \cdot \frac{B}{G_B} \quad (5.17)$$

$$\frac{dC}{dL} = [-k_X C^2S - k_Y CX + k_C C_1] \frac{B}{G_B} \quad (5.18)$$

On the basis of the energy balance, equation (5.19) can be written for the burden temperature in the fourth section and the gas temperature is again given by equation (5.10).

$$\begin{aligned} \frac{dT_m}{dL} = \frac{1}{C_{Pm} G_S} [& \alpha_2 (T_g - T_m) + \alpha_3 (T_w - T_m) - \Delta H_{C1} B k_C C_1 \\ & + \Delta H_X B k_X C^2S] \end{aligned} \quad (5.19)$$

The temperatures of the inside and outside walls are obtained from an overall heat balance equations (5.20) to (5.23).

$$\alpha_1(T_g - T_w) + \alpha_3(T_m - T_w) + \alpha_4(T_{w'} - T_w) = 0 \quad (5.20)$$

$$\alpha_4(T_w - T_{w'}) + \alpha_5(T_a - T_{w'}) = 0 \quad (5.21)$$

$$T_w = \frac{(\alpha_1 T_g + \alpha_3 T_m + \alpha_4 T_{w'})}{(\alpha_1 + \alpha_3 + \alpha_4)} \quad (5.22)$$

$$T_{w'} = \frac{(\alpha_5 T_a + \alpha_4 T_w)}{(\alpha_4 + \alpha_5)} \quad (5.23)$$

Equations (5.6) through (5.23) establish the mathematical form which represents the behaviour of the cement rotary kiln. Similarly equations (5.6) through (5.14) together with equations (5.19) after deleting the last term corresponding to lime-silica reactions represent the behaviour of a rotary lime sludge kiln.

The above equations are used in the computer program to predict the temperature and composition profiles in cement and lime sludge rotary kilns. A list of the input variables required as data and the output parameters of the program is shown in Table 5.3 and a flow chart for the simulation program is depicted in Figure 5.1.

TABLE 5.3: INPUT/OUTPUT PARAMETERS FOR SIMULATION PROGRAM

Input Variables	Definition
L	Overall length of kiln
L_C	Chain section length
G_B	Product mass flow rate
G_N	Nitrogen mass flow rate
C_{Pg}	Specific heat of gas
C_{Pm}	Specific heat of burden material
ϵ_m	Emissivity of burden material
ϵ_g	Emissivity of gas
ϵ_w	Emissivity of wall
T_a	Ambient temperature
$T_g(0)$	Exit gas temperature
$T_m(0)$	Inlet slurry temperature
$C_1(0)$	CaO as $CaCO_3$ in raw feed/unit clinkerable mass
$W(0)$	Water in slurry feed/unit clinkerable mass
$C'(0)$	CO_2 /unit N_2 mass in exit gas
$W'(0)$	Water/unit N_2 mass in exit gas
$S_1(0)$	SiO_2 in raw feed/unit clinkerable mass
B	Clinkerable burden mass/unit length
IS	Integration step size
A_i	Heat transfer areas
k_w	Thermal conductivity of wall
L_f	Flame length
RF	Rate of combustion/unit length of burning zone

Table 5.3 (contd)

Output Variables	Definition
$T_g(x)$	Temperature of gas at any length x
$T_m(x)$	Temperature of burden material at any length x
$W(x)$	Water/unit clinkerable mass at any length x
$Cl(x)$	CaO as $CaCO_3$ /unit clinkerable mass at any length x
$C(x)$	Free line/unit clinkerable mass at any length x
$X(x)$	C_2S /unit clinkerable mass at any length x
$Y(x)$	C_3S /unit clinkerable mass at any length x
$G_S(x)$	Total burden mass/unit clinkerable mass at length x
H_{vap}	Total heat consumed in vaporisation of water till length x
H_{calc}	Total heat required for calcination till length x
H_{loss}	Total heat loss till length x

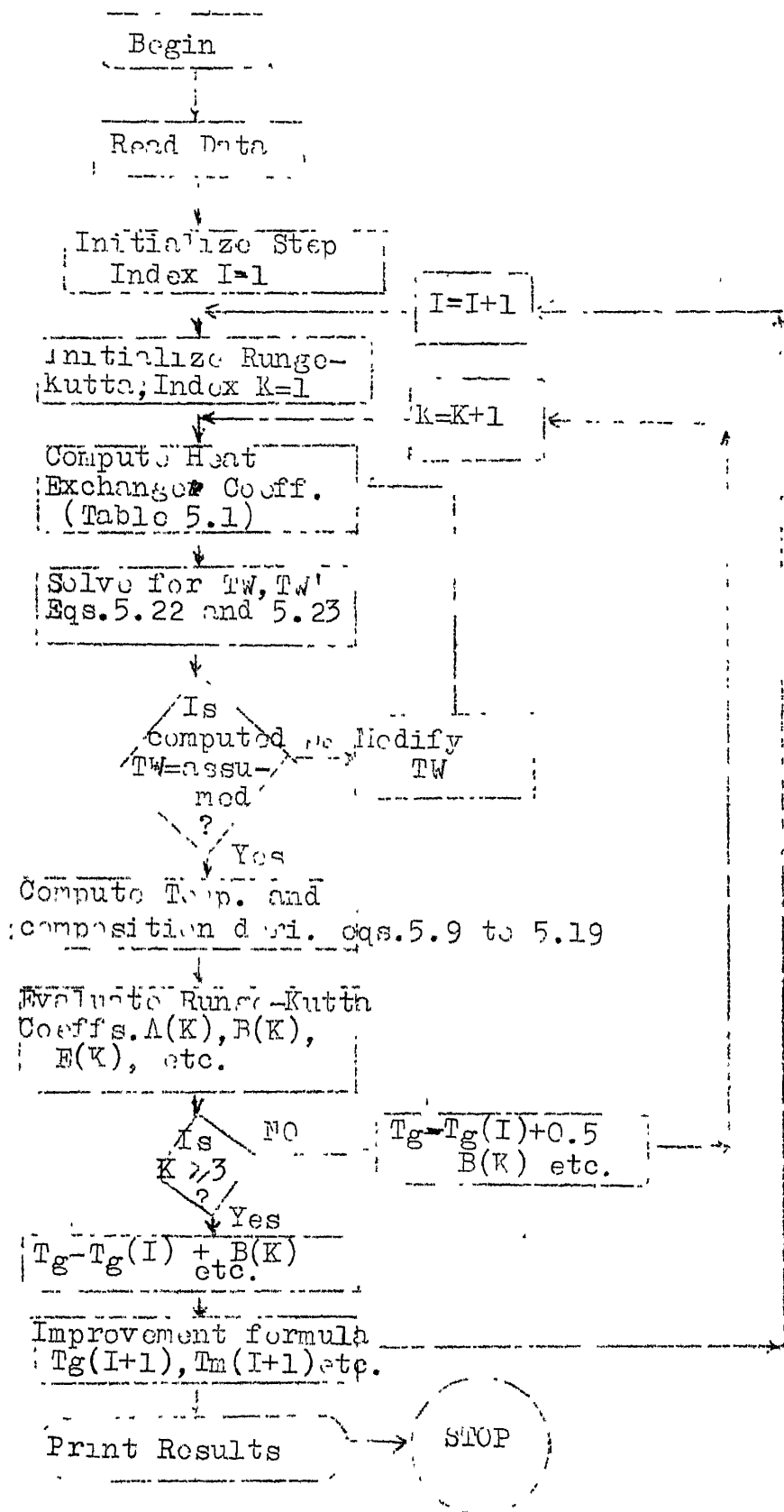


FIG.5.1: FLOW CHART FOR SIMULATION PROGRAM

CHAPTER 6

APPLICATIONS OF THE MODEL

The model developed in Chapter 5 was tested for the wet process cement kiln and lime sludge kilns using operating data from manufacturers/kiln operators as well as data reported in literature. In some cases manufacturers were only able to give a partial characterization of their kilns and it was necessary to rely upon literature indicated values for kilns in similar size range producing the same product. Table 6.1 summarises the data obtained from various sources. Data on cement kilns were obtained from A.C.C. Limited, Bombay, K.C.P. Limited, Madras, and also taken from literature Lyons et al [41]. Data for lime sludge kilns were provided by West Coast Paper Mills, Ltd., Karnataka and also taken from literature Libby [40]. Data obtained from Central Pulp Mills Ltd., Surat for a limestone rotary kiln are also included in Table 6.1.

A DEC-10 computer was used to solve the system of simultaneous differential equations developed for the model. The computer program listing is given in Appendix B. The **model is first applied** to the relatively simpler lime sludge kilns and later used with the three sets of data for the cement kilns. Computer outputs for data from West Coast Paper Mills, Karnataka and A.C.C. Limited, Bombay are attached. Simulated profiles of the burden composition and

gas and burden temperatures for all five sets of data are shown in Figures 6.1 to 6.5. Summary of simulation results for each of the five data sets are shown in Tables 6.2 to 6.6.

6.1 Discussion of Results:

The model developed in Chapter 5 considers two subdivisions for the drying zone. For the purpose of the model it was assumed that the gas temperatures during evaporation were high enough and consequently that the rate of liquid evaporation was controlled by heat transfer rates rather than mass transfer rates. The model was able to predict drying zone lengths fairly accurately. However, the temperature of the burden material is not constant at exactly 100°C as predicted by the model. Investigations on rotary cement kilns [5] show that the temperature of the material in the drying zone remains constant only until a moisture content of 4 per cent reached. Upto this point the surface of the material remains moist. Water held at the surface by capillary action and adsorption is evaporated only when the moisture content falls below 4 per cent. In the drying of cement slurry in the chain section of rotary kilns, the raw mix becomes plastic at 13-16 per cent moisture content and there occurs another transition point. In all wet process cement rotary kilns, the drying rate in the chain zone above 13-16 per cent moisture content is higher than that below it.

In the region where the slurry is liquid the chains are completely covered with slurry exposing a large surface area and consequently a high drying rate. On the other hand, in the plastic state of the raw mix, the chain system functions as a regenerative heat exchanger; the chain becomes heated in the gas stream and the heat they thus absorb is imparted to the kiln charge when they dip into the layer of material. In the absence of data for drying rates in the three zones, above 13-16 per cent, between 13-16 per cent and 4 per cent, and below 4 per cent moisture content it has not been possible to model the drying phenomenon in wet process rotary kilns with any degree of refinement.

The decarbonation of the raw meal in cement rotary kilns according to the model starts when the burden temperature reaches 887°C (1629°F) as in Figures 6.1 to 6.3. However, in actual practice it has been found that the dissociation of calcium carbonate already begins at a material temperature of about 600°C (1112°F). At the start of decarbonation no liberated lime can be determined as it combines immediately with the silica and alumina of the clay. Therefore, not more than 2 per cent free lime [5] is present at temperatures up to 800°C (1472°F).

The formation of new phases in the rotary kiln at relatively low temperatures can be attributed to the fact that the surface of the material exposed to the radiation

of the flame is considerably hotter than the measured average temperature of the charge material. The first decomposition of calcium carbonate occurs at the surface of the material exposed to the radiation of the flame. In consequence of the rotation of the kiln the decomposed material mingles with the rest of the material, and its temperature equals the average measured temperature of the charge. Weber's [5] measurements have shown that the temperature of the surface exposed to the flame is roughly 200°C hotter than the general mass of material. This partly explains why calcium carbonate decomposition in kilns appears to start at roughly 600°C instead of 887°C which is the normally observed value. The equations used in the model describing the process were based on the assumption that at a given cross-section in the kiln, the gas, solid, inner-wall and outer-wall temperatures were independent of their radial position. For the solids, this assumption is equivalent to stating that the material is well mixed. It is theoretically possible to take into account the heat transfer resistance between the burden surface and the burden interior. However, Pearce's [1] equation to calculate the 'solid side coefficient' have variables which have not been determined for commercially operating kilns. In view of this, complete mixing was assumed for the model in line with the assumption of Imber and Paschkis [3].

Another reason why decarbonation in actual kilns appears to start before that predicted by the model is that there is carryover of kiln dust by the gases. The quantity of dust carried increases with the velocity of gas. This leads to some sort of 'axial mixing' for the burden material. Decarbonated material carried by the gas is precipitated by the chains and heat exchanger inserts at the drying end of the kiln. In view of this, the apparent decarbonation at any axial distance from the feed end predicted by the model is slightly lower than that in an actual kiln where there is 'axial mixing'.

The simulated profiles for C_2S and C_3S in Figures 6.1 to 6.3 do not show a sharp peak as is observed in practice. This peak occurs in an actual kiln because 20-30 per cent of the burden material becomes molten at the clinkering temperature when reaction rates increase substantially compared to solid-solid reactions. Some of the parameters that control the mass transfer during clinkering are the mineralogy of the raw materials, the fineness of the raw materials, and the homogeneity of the mix. Therefore, it is very difficult to describe the kinetics of clinker formation in a general manner. At temperatures greater than $1300^{\circ}C$ ($2372^{\circ}F$), the fineness and homogeneity of the raw mix are the rate controlling parameters. Since data on the sieve analysis and homogeneity of the raw mix before

clinkering are not available further refinement in the model for the reaction between CaO particles and cement clinker is not possible.

For the lime sludge kilns Figures 6.4 and 6.5 show that the flame length has been ignored because lime kilns utilize natural gas or oil as fuel which gives a short intense flame.

Figures 6.6 and 6.7 show typical improvements in heat efficiency that can be obtained by reducing the slurry water content (with constant feed rate of slurry). Figure 6.6 is for a cement rotary kiln at KCP Limited, Madras and Figure 6.7 is for data from West Coast Paper Mills, Karnataka for their lime-sludge kiln.

CHAPTER 7

CONCLUSIONS AND RECOMMENDATIONS

7.1 Conclusions

1. The model developed in the present study was applied to actual operating cement and lime sludge kilns and gave fairly good agreement (within 8.1 per cent) for the enthalpy balance. The drying zone lengths predicted by the model were within 13 per cent of actual values in all cases.

2. A maximum error of 14.4 per cent in the length of the calcining zone as predicted by the model was mainly attributable to : (a) the assumption of perfect mixing in the burden material and (b) 'axial mixing' because of fine dust particles of decarbonated material being carried by the gas and precipitated by the chains at the drying end of the kiln.

3. It was also observed that simulated profiles for C_2S and C_3S did not show a sharp peak at clinkering temperature as observed in practice. This peak occurs in the actual kilns because 20-30 per cent of the burden material becomes molten at clinkering temperature thus increasing the rates of reaction compared to solid-solid reactions.

7.2 Recommendations

The present work could be very well applied to the simulation of lime stone kilns. The principal difference that arises in the design of rotary kilns for limestone as compared to that of lime sludge kiln is due to the size of the particles (5-20 cm in diameter) which contributes a major resistance to heat transfer. Calcination of limestone takes place in a very narrow zone which is the phase boundary between calcium oxide and calcium carbonate. In view of this, the rate of calcination becomes an important factor in the design of rotary kilns for limestone. It has been found [45] that the length of time required to calcine is directly proportional to the particle size. Using this assumption a two-dimensional model could be very well applied in the present work for lime stone kilns.

TABLE 6.1: ROTARY KILN DATA SUPPLIED BY CEMENT/LIME MANUFACTURERS

KILN DATA	CEMENT KILNS			LIME SLUDGE KILNS			LIME STONE KILN	
	KCP	ACC	LYONS[41]	WEST COAST	LIBBY	[40]	CENTRAL PULP MILLS	
Length, ft	443	368	450	181	300		170	
I.D., ft.	11.81	6.6x8x9	10.25	8.2	7.0		4.6	
O.D., ft	11.97	10x9x10	12.00	-	8.0		8.6x9.2	
Chain section, ft	115	56	100	-	-		12	
OPERATING DATA								
Production, tons/day	650	300	608	40	100		47	
Speed, rev/min	1.2	0.86	-	0.4-1.0	-		1.5	
Slurry water, per cent	35	35	36	57	39.5		0.6	
Slurry temp. °F	Ambient	95	40	158	70		Ambient	
Exit gas temp., °F	482	356	500	419	400		530	
Exit burden temp., °F	2462	446 ^a	2500	1655	2566		1900	^a Exit temperature from clinker
Clinker free lime percent	0.8	1.5	0.5	-	-		-	cooler
Fuel type	coal	coal	coal	oil	gas		oil	
Fuel rate, Btu/hr	168x10 ⁶	73.2x10 ⁶	179x10 ⁶	18.2x10 ⁶	35x10 ⁶		24.3x10 ⁶	
Approx zone length, ft	131	69	100	43	60		43	
(a) Drying	125	95	125	85	160		85	
(b) Calcining	-	-	33	-	-		-	
(c) Burning	-	16	20	13	14		-	
Heat loss, /	-	3	3.5	4-4.5	-		-	
Residence time, 2.66								

TABLE 6.2: SIMULATION OF ROTARY CEMENT KILN (ACC LTD)Kiln Data

Length, ft.	368
I.D. of kiln, ft	6.6x8x9
O.D. of kiln, ft	10x9x10
Chain section, ft	56

	Zone Lengths		Per cent error
	Actual Value	Simulated Value	
Drying zone	69	78	+13
Calcining zone	98	85	-13.2

Heat Balance (Reference temperature 95°F)Input

	Btu/hr
Fuel	67.23×10^6
Input gas 67,200 lbs/hr at 646°F	11.71×10^6
	<u>78.94×10^6</u>

Output

Solids 28,000 lbs/hr at 2053°F	14.25×10^6
Gas to stack 106,960 lbs/hr at 356°F	8.79×10^6
Latent heat of vaporization 24080 lbs/hr of water	23.30×10^6
Latent heat of calcining and clinkering	19.20×10^6
Heat losses	13.40×10^6
Total	<u>78.94×10^6</u>

Cooler Correction

Total input	78.94×10^6
Heat recuperated by cooler (solids 2046°F - 432°F)	<u>11.71×10^6</u>
Net fuel	<u>67.23×10^6</u>
Actual fuel input	73.21×10^6
Per cent deviation in energy balance	8.16 per cent

TABLE 6.3: SIMULATION OF CEMENT ROTARY KILN LYONS [41]

Kiln Data

Length, ft.	450
I.D. of kiln, ft	10.25
O.D. of kiln, ft	12
Chain section, ft	100

	<u>Zone lengths</u>		Per cent error
	<u>Actual value</u>	<u>Simulated value</u>	
Drying zone	100	111	+11
Calcining zone	125	107	-14.4

Heat Balance (Reference temperature 40°F)

<u>Input</u>	<u>Btu/hr</u>
Fuel	174.10×10^6
Input gas 229,000 lbs/hr at 502°F	$\frac{33.50 \times 10^6}{207.60 \times 10^6}$
<u>Output</u>	
Solids 56,900 lbs/hr at 2573°F	37.47×10^6
Gas to stack 309,700 lbs/hr at 490°F	44.88×10^6
Latent heat of vaporization 49,700 lbs/hr, of water	48.10×10^6
Latent heat of calcining and clinkering	38.80×10^6
Heat losses	$\frac{36.80 \times 10^6}{206.06 \times 10^6}$
<u>Cooler Correction</u>	
Total input	207.60×10^6
Heat recuperated by cooler (solids 2573°F-303°F)	$\frac{33.50 \times 10^6}{174.10 \times 10^6}$
Actual fuel input	179.00×10^6
<u>Per cent deviation in energy balance</u>	<u>3 per cent</u>

TABLE 6.4: SIMULATION OF ROTARY CEMENT KILN (KCP LTD)

Kiln Data

Length, ft	443
I.D., ft	11.81
O.D., ft.	11.97
Chain section, ft	115

	Zone lengths		per cent error
	Actual value	Simulated value	
Drying zone	131	131	0
Calcing zone	125	110	-12.0

Heat Balance (Reference Temperature 95°F)

<u>Input</u>	<u>Btu/hr</u>
Fuel	157.17×10^6
Input gas 155000 lbs/hr at 753°F	32.13×10^6
	189.30×10^6
<u>Output</u>	
Solids 60,600 lbs/hr at 2566°F	38.78×10^6
Gas to stack, 240,000 lbs/hr at 482°F	29.31×10^6
Latent heat of vaporization of 52,264 lbs/hr of water	50.70×10^6
Latent heat of calcining and clinkering	41.50×10^6
Heat losses	29.00×10^6
Total	189.29×10^6
<u>Cooler correction</u>	
Total input	189.29×10^6
Heat recuperated by cooler (solids 2566°F - 527°F)	32.12×10^6
	157.17×10^6
Actual fuel input	168.00×10^6
Per cent deviation in energy balance	6.4 per cent

TABLE 6.5: SIMULATION OF LIME SLUDGE KILN LIBBY [40]Kiln Data

Length, ft	300
I.D., ft	7.00
O.D., ft	8.00
Chain section	-

	<u>Zone lengths</u>		Per cent error
	<u>Actual value</u>	<u>Simulated Value</u>	
Drying zone	60	59	-1.6
Calcining zone	160	150	-6.25

Heat Balance (Reference temperature: 70°F)

<u>Input</u>	<u>Btu/hr</u>
Input gas 28,700 lbs/hr at 3917°F	34.65×10^6
<u>Output</u>	
Solids 9300 lbs/hr at 2566°F	4.14×10^6
Gas to stack 45,562 lbs/hr at 400°F	4.74×10^6
Latent heat of vaporization of 10,308 lbs/hr of water	10.10×10^6
Latent heat of calcining	10.60×10^6
Heat losses	4.87×10^6
Total	34.56×10^6
Actual fuel input	35.00×10^6
Per cent deviation in energy balance	1 per cent

TABLE 6.6: SIMULATION OF LIME SLUDGE KILN
(West Coast Paper Mills)

Kiln Data

Length, ft.	181
I.D., ft.	8.2
O.D., ft.	-
Chain section, ft.	-

	<u>Zone lengths</u>		<u>Per cent error</u>
	<u>Actual value</u>	<u>Simulated Value</u>	
Drying zone	43	47	+9.3
Calcining zone	85	79	-7.0

Heat Balance (Reference temperature 158°F)

<u>Input</u>	<u>Btu/hr</u>
Input gas 14,500 lbs/hr at 3058°F	178.20 x 10 ⁵
<u>Output</u>	
Solids, 3,740 lbs/hr at 1655°F	14.56 x 10 ⁵
Gas to stack, 25100 lbs/hr at 419°F	20.64 x 10 ⁵
Latent heat of vaporization of 8066 lbs/hr of water	78.40 x 10 ⁵
Latent heat of calcining	41.20 x 10 ⁵
Heat losses	23.50 x 10 ⁵
	<u>178.30 x 10⁵</u>
Actual fuel input	18.2 x 10 ⁶
Percent deviation in energy balance	2.2 per cent

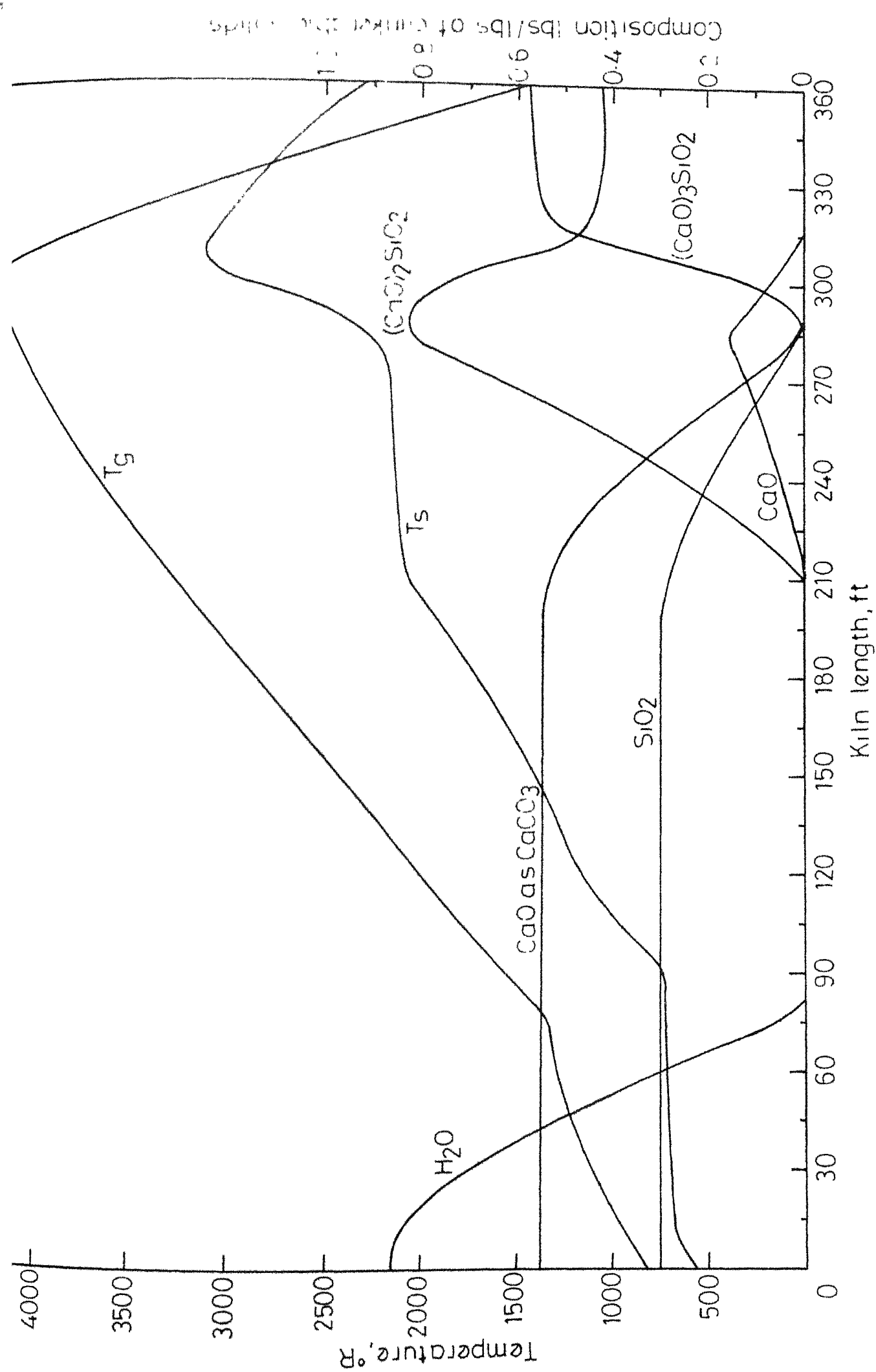


Fig 6.1 - Temperature and composition profiles for cement kiln (ACC - LTD)

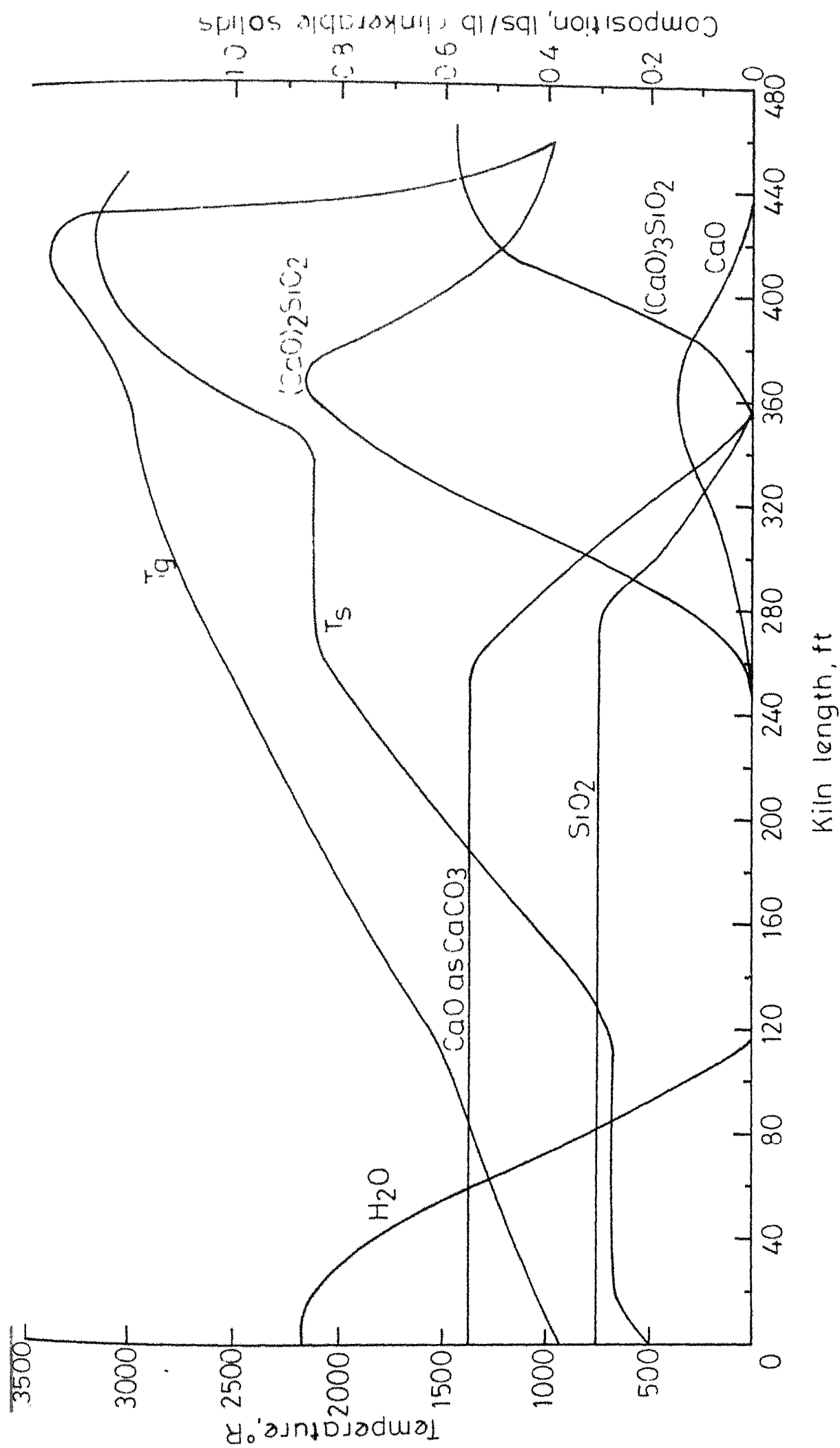


Fig 6.2 - Temperature and composition profiles for cement kiln (LYONS et al [41])

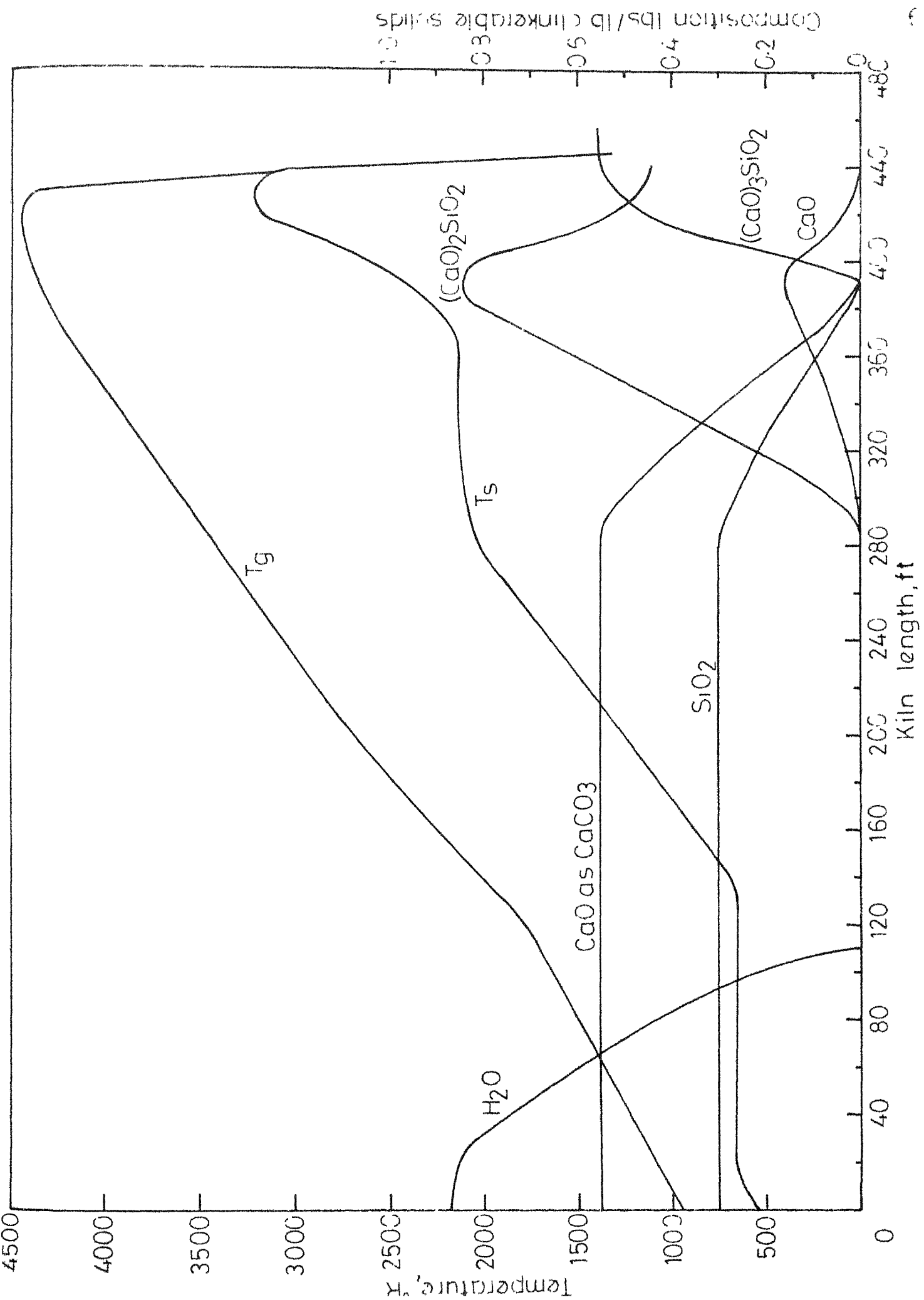


Fig 6.3 - Temperature and composition profiles for cement manufacturing.

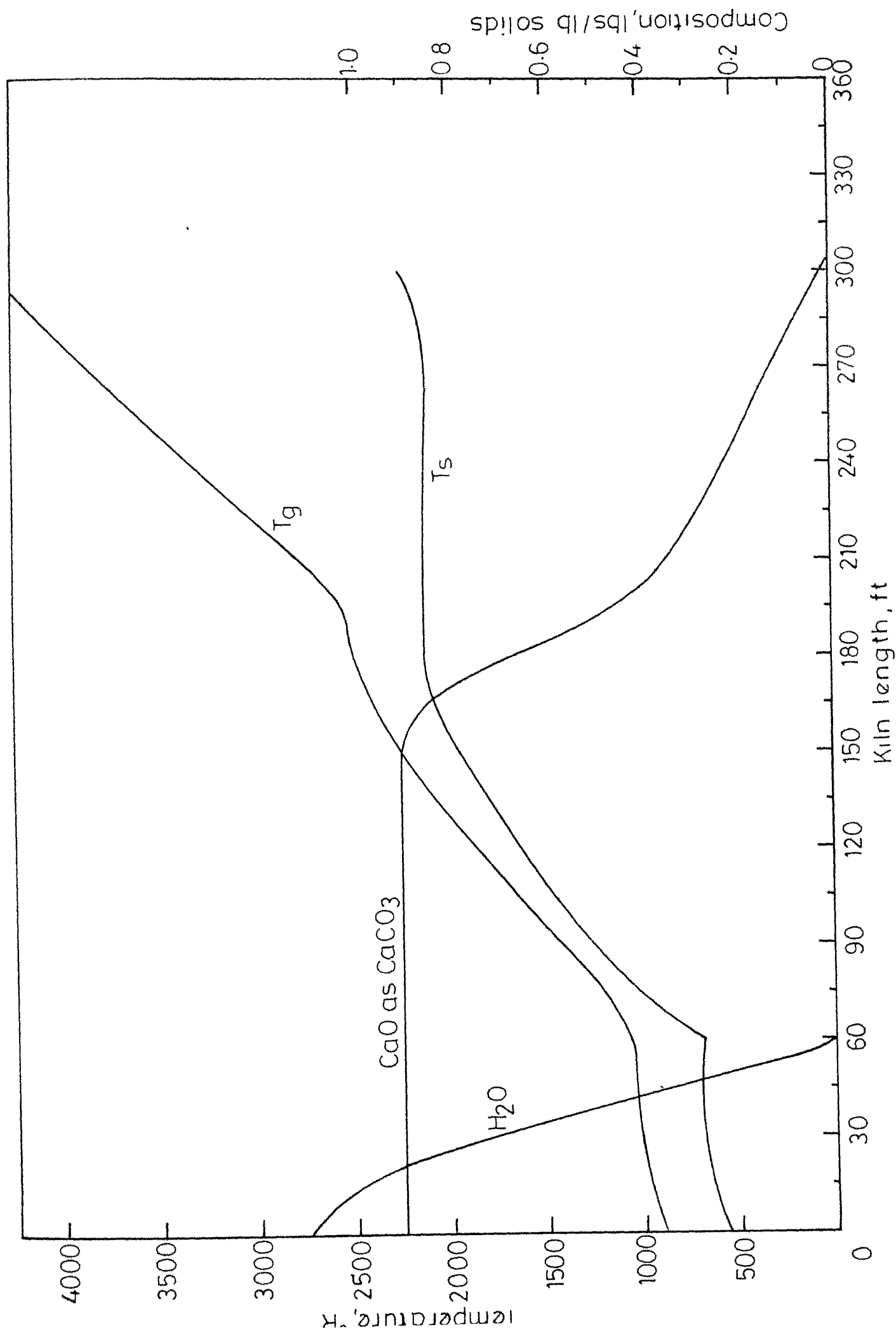


Fig 6.4 -Temperature and composition profiles for lime sludge in (L'BBY[40])

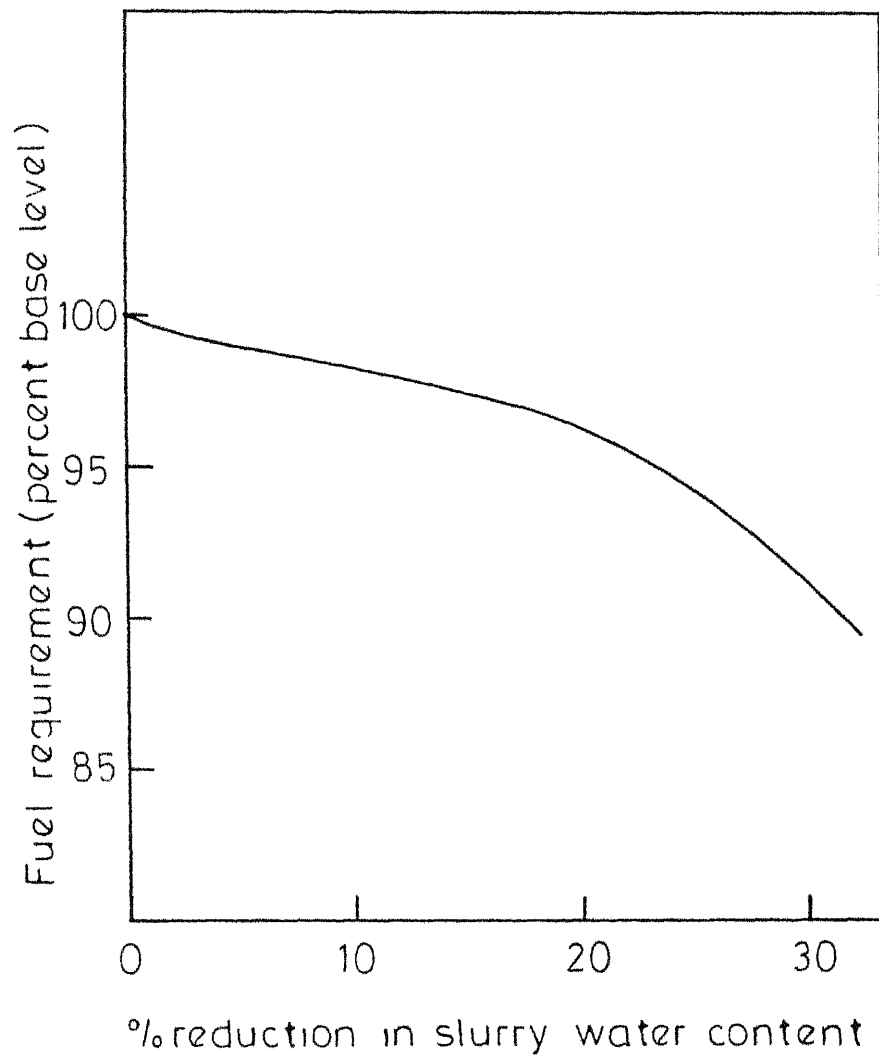


Fig 6.6 - Influence of cement raw mix moisture on fuel requirement (KCP-LTD)

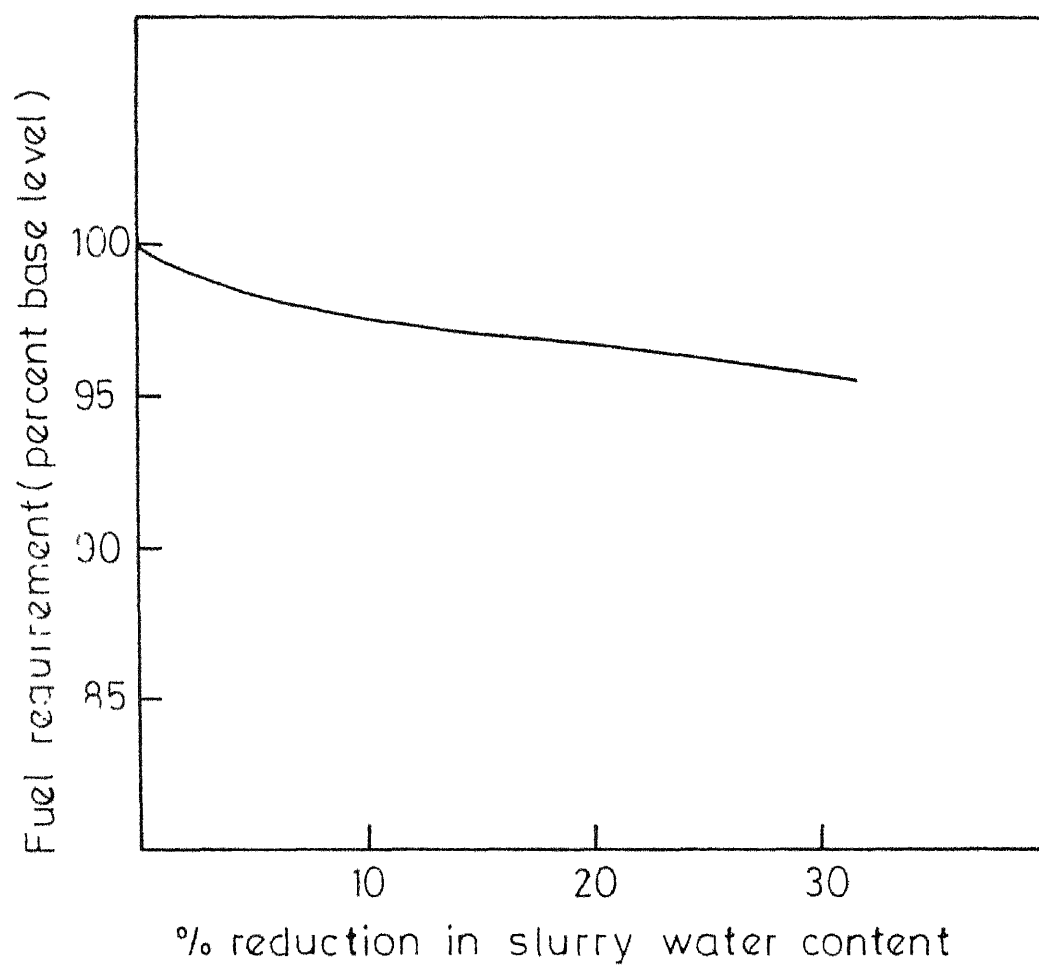


Fig 6 7 - Influence of lime sludge moisture on fuel requirement (West Coast Paper Mills)

BIBLIOGRAPHY

1. Pearce, K.W. 'A Heat Transfer Model for Rotary Kiln'
4th Flames in Industry Symposium, London (1972).
2. Pearce, K.W. 'Rotary Kiln Fuel Economy in Minerals
and Refractories Processing'
I.Chem.E. Symposium Series 43 (1973).
3. Imber, M. and Paschkis, V. 'A New Theory for a Rotary Kiln Heat
Exchanger'
Int. Journal of Heat Transfer 5: 623 (1962).
4. Sullivan, J.D. et al. 'Passage of Solid Particles through
Rotary Cylindrical Kilns'
Bureau of Mines Tech. Paper 384,
Washington (1927).
5. Weber, P. 'Heat Transport in Rotary Kilns'
Bauverlag GmbH, Weisbaden, Berlin (1963).
6. Folliot, A. 'Heat Transmission in the Rotary Cement
Kiln'
Centre d Etudes et de Rech
de Ind. des Liants Hydrauliques,
Pub.Tech.No.70, Paris (1955).
7. Gygi, H. 'Thermodynamics of the Cement Kiln'
Proc. of 3rd International Symposium on
the Chemistry of Cements, London (1952),
London (1954).
8. Gygi, H. 'Heat Technological Investigations on
the Rotary Kiln for Making Cement Portland
Clinker'
Thesis, Zurich (1936).
9. Martin, G. 'Chemical Engg. and Thermodynamics Applied
to the Cement Rotary Kiln', London (1932).
10. Krischer, O. 'The Scientific Principles of Drying
Technique'
Berlin (1956).
11. Kroll, K. 'The Processes in Rotary Driers and
Heaters for Free Flowing Material'
Berlin (1950).

12. Anselm, W. 'The Rotary Kiln-Determination of Dimensions and Model Similarity' Zement-Kalk-Gips 6(5):151 (1953).
13. Anselm, W. 'Considerations on the Model Similarity of Rotary Kilns' Tagungsberichte der Zementindustrie, (11):1 (1955).
14. Modl, E. 'Rational Model Analysis of Fuel-Fired Industrial Furnaces', Technische Mitteilungen 45(11):388 (1952).
15. Bergkamp, E. S. 'Model Analysis of Rotary Kilns-General Principles', Tagungsberichte der Zementindustrie (11):5 (1955).
16. Eigen, H. 'Contribution to the Model Analysis of Cylindrical Rotary Kilns', Zement-Kalk-Gips 7(11):434 (1954).
17. Saeman, W.C. Chem. Engg. Progress p 508 (1951).
18. Boguslavskii, N.M. Khim. Prom (2):89 (1956).
19. Ronco, J.J. Industria y Quimica 20:605 (1960).
20. Baranowskii, W.U. Tsevt. Metal 6: 56 (1962).
21. Khodorov, E.P. 'The movement of Materials in Rotary Kilns' Moscow (1957).
22. Bayard, R.A. Chem. and Metall. Engg. 52:100 (1945).
23. Zablotny, W.W. 'The movement of Charge in Rotary Kilns' Int. Chem. Engg. 5(2):360-366 (1965).
24. Lea, F.M. and Desch, C.H. 'The Chemistry of Cement and Concrete' (2nd Ed), Arnold, London (1956).
25. Bogue, R.H. 'Proc. of the International Symposium on the Reactivity of Solids' Gothenburg (1952).
26. Torpov, N.A. and Luginina, I.G. Tsement 19 (1), (4) (1953).
27. Woermann, E. 'Proc. of the 4th International Symposium on Chemistry of Cements', pp 104-119, National Bureau of Standards Monograph 43, U.S. Department of Commerce.

28. Jander, W. 'Z. Angew. Chem.' 51: 696 (1938).
29. Johanson, O.K. and Jour. Amer. Chem. Soc., 56:2327 (1934).
Thorvaldson, T.
30. Kuhl, H. and 'The Binding of Lime by the Constituents
Lorenz, H. of the Clay During the Progressive Heating
of the Cement Raw Material'
Zement 8(19):604 (1929).
31. Weyer, I. 'The Course of the Reaction of Kaolin and
lime on Static Heating',
Doctoral Thesis, Kiel (1930).
32. Keyser, W.L. 'Reactivity in the Solid State Between
the Oxides of the Cement System'
Tidskr. for teknisk-vetenskapl forskning
26(7):292 (1955).
33. Wachters, L.H.J. 'The Calcining of Sodium Bicarbonate in a
and Kramers, H. Rotary Kiln', 3rd European Symposium
Chem. Reaction Engg. Amsterdam (1964).
34. Schack, A. 'Industrial Heat Transfer' (5th Ed)
Dusseldorf (1957).
35. Heilgenstaedt, W. 'Heat Technological Calculations for
Industrial Furnaces' (3rd Ed.)
Dusseldorf (1951).
36. Grober, E. and 'The Fundamental Laws of Heat Transmission'
Grugull, U. (3rd Ed.) Berlin (1955).
37. Rhuland, W. 'Investigations of Flames in the Cement
Rotary Kiln',
Journ. Inst. Fuel, (2):69 (1967).
38. Hottel, H.C. 'Radiative Heat Transfer'
and Sarafin, A.F. McGraw Hill, New York (1967).
39. Sass, A. 'Simulation of Heat Transfer Phenomena
in Rotary Kilns', Ind. and Engg. Chem.
(PDD) 6:532 (1967).
40. Libby, C.E. 'Pulp and Paper Science and Technology'
McGraw Hill, New York (1962).

41. Lyons, J.W.
et al. Ind. and Engg. Chem., PDD, 1(1):29(1962).
42. Lacey, W.N.,
et al. Ind. and Engg. Chem. (Ind.Ed), 21:124
(1929).
43. Lacey, W.N. Ind. and Engg. Chem. (Ind. Ed), 24:332
(1932).
44. Heilmann, T. Chemistry of Cement, Proc. of the 4th
International Symposium, Washington
(1960).
45. Furnas, C.C. Ind. and Engg. Chem. 22:721 (1930).
46. Diomidovskii 'Furnaces in Non Ferrous Metallurgy'
Moscow (1956).

APPENDIX ATHE CHEMISTRY OF LIME AND CEMENTPortland Cement:

Portland cement is a powdered mixture containing mainly dicalcium and tricalcium silicates, and small amounts of calcium aluminates. In all applications it is slurried in water and sets slowly bonding intermixed aggregates into a hardened mass of concrete. It is made by sintering a mixture of calcareous and argillaceous raw materials. Natural calcareous deposits like limestone and shell beds supply lime while natural argillaceous deposits like clay, shale, slate deposits are sources of both silica and alumina. The principal raw materials, lime, silica and alumina should be in the desired proportion in the raw mix for cement production. Supplemental materials of suitable composition may be used to adjust the raw mix to the desired proportion of ingredients. Among other compounds occurring in natural deposits iron is an important constituent. It combines with lime and/or alumina to form lime-alumina-iron compounds and also acts as a flux. Phosphates and alkalies are present in small amounts as impurities while magnesia may be present in varying proportions in some raw materials. During the sintering process chemical reactions take place producing nodules, (clinkers) which are composed principally of calcium silicates and aluminates.

ASTM (Amer. Soc. of Testing Materials) has classified Portland cement in five categories as shown in Table A.1, which also shows the average composition of the major constituents.

A.2 Reactions in the Cement Rotary Kiln:

Reactions in cement rotary kilns occur in three or four zones depending on whether it is a dry or a wet process kiln. Lea [24], Bogue [25], Torpov and Luginina [26], Woermann [27] and several others have studied cement reactions extensively. Information on the course of reactions in commercial kilns has been obtained by sampling at various points, either after stopping the kiln and allowing it to cool [42] or, better during normal operations [43]. Temperatures at various points can be determined by inserting thermocouples through the lining. The reactions occur in stages as in Table A.2, according to Lea [24]. There is considerable overlap in these processes caused by variations in mineralogy of raw materials, particle size distribution and homogeneity of the raw mix.

Various authors are in general agreement [5,25] with the equations listed in Table A.2 and differ in the exact sequence of reactions by which the cement compounds are formed. It was at one time generally supposed that the cement compounds were formed almost wholly by crystallization from the liquid and that little or no interaction occurred before melting

12

TABLE A.1: ASTM CLASSIFICATION OF CEMENTS AND
AVERAGE COMPOSITION

Designation	General description	Potential compound ^a , per cent			
		C ₃ S	C ₂ S	C ₃ A	C ₄ AF
Type I	Normal (General purpose)	49	25	12	8
Type II	Modified (General purpose)	46	29	6	12
Type III	High early strength	56	15	12	8
Type IV	Low-heat	30	46	5	13
Type V	Sulphate resisting	43	36	4	12

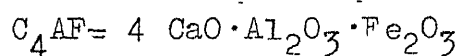
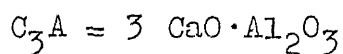
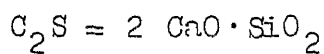
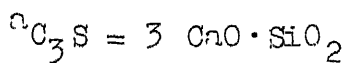


TABLE A.2: REACTIONS IN A ROTARY CEMENT KILN

Temperature, °C	Process	Thermal Change
100°	Evaporation of free water	Endothermic
>500°	Dehydroxylation of clay minerals	Endothermic
>900°	Crystallisation of products of clay mineral dehydroxylation Decomposition of CaCO_3	Exothermic
900-1200°	Reaction between CaCO_3 or CaO and aluminosilicates	Exothermic
1250-1280°	Beginning of liquid formation	Endothermic
1280°	Further liquid formation and formation of cement compounds	Probably endothermic

started; but Bogue [25] has suggested that reaction of the constituents in the solid phases as well as with the melt constituents are also important.

The maximum temperature of 1300-1500°C is reached in the 'burning zone' at the hot end of the kiln. The clinkering temperature is chosen so as to produce a degree of melting sufficient to cause the material to cohere into small ball or lumps of clinker. At this temperature 20-30 per cent of the material is normally molten. Overburning, i.e. operating at a higher temperature, is generally considered undesirable, as it leads to difficulties in running the kiln and possibly yields a less reactive product, owing to the formation of larger crystals on ones containing fewer defects. Beyond the burning zone the temperature falls and the clinker enters the cooler at 1000-1300°C. The mixture takes about 2.5 hours to pass through a kiln 60 m long. Studies on the analysis of clinker [5] show that the content of free lime rises to a maximum at a point somewhat before the burning zone. This suggests that at 900-1000°C decomposition of the CaCO_3 occurs more rapidly than the reaction of the resulting CaO with alumina silicates. Immediately before the burning zone the free CaO content drops again and the temperature rises sharply to about 1250°C. Both effects are caused by the exothermic reaction of the CaO with the alumina silicates. The mixture then passes through the

burning zone at 1300-1500°C, where the reaction is completed and the free CaO drops almost to zero.

The product at the clinkering stage consists essentially of crystals of C_3S and C_2S and a liquid containing CaO with all or most of the Al_2O_3 , Fe_2O_3 and MgO, but relatively little SiO_2 . The aluminate and ferrite phases therefore only form during cooling. Other processes that occur during cooling include polymorphic transitions especially in C_2S and reaction between the liquid and the C_3S or C_2S crystals already formed. The latter step alters the ratio of C_3S to C_2S in the final clinker.

Alumina and iron oxide serve as flux during cement burning; without them the silicates could only be formed at much higher temperatures or in much longer times. The relations between the Al_2O_3/Fe_2O_3 weight ratio of the mix and the amounts of liquid formed at different temperatures are discussed by Lea [24]. At a clinkering temperature of 1400°C rather more liquid is formed for each per cent of Al_2O_3 than of Fe_2O_3 , but this situation can be reversed in the earlier stage of liquid formation below 1300°C. There is also some evidence that Fe_2O_3 can be more effective in promoting solid-solid reactions.

Successful burning of cement depends not only on the composition of the raw mix but also on the reactivity which is largely dependent on the fineness and the state of

crystallinity of individual minerals; defects in a crystal are likely to make it more reactive. Torpov and Luginina [26] investigated the influence of particle size of the raw mix on the processes of combination in calcium oxide in Portland cement burning. They showed that care had to be taken to prevent the fine material from remaining in the clinkering zone too long, to avoid the formation of rings in the kiln. They later investigated the effect of rapid burning, which accelerated the combination of raw materials. Heilmann [44] showed that not more than 0.5 per cent of silica particles above 0.2 mm nor more than 1 per cent between 0.09 and 0.2 mm should be present in raw mixes with a lime saturation factor as high as 0.95, but for lower lime saturation factors twice these amounts might be allowed. Upto 5 per cent of pure calcite particles greater than 0.15 mm in size can be tolerated while impure silaceous limestones of greater size can be used without detrimental effects.

APPENDIX B

COMPUTER PROGRAM LISTING

```

0100 C *****
0200 C SIMULATION OF A ROTARY KILN FOR THE SLAGGE
0300 C *****
0400 C THE FOLLOWING ALGORITHM FOR THE DIGITAL SIMULATION OF A KILN
0500 C SLAGGE KILN EMPLOYS THE FOURTH ORDER "RUNGE-KUTTA METHOD" WITH
0600 C KUTTA'S COEFFICIENTS TO INTEGRATE A SYSTEM OF FIVE SIMULTANEOUS
0700 C FIRST ORDER DIFFERENTIAL EQNS. FOR MASS & HEAT TRANSFER IN A
0800 C ROTARY KILN, ACROSS A STEP OF LENGTH "S" IN THE INDEPENDENT VAR-
0900 C IABLE "L", SUBJECT TO INITIAL CONDITIONS. EACH OF THE TEMPERATURE
1000 C & COMPOSITION DERIVATIVES MUST BE COMPILED FOUR TIMES PER INTEG-
1100 C RATION STEP. "I" IS THE STEP COUNTER FOR EACH INTEGRATION STEP
1200 C AND EQUALS 1 AT THE END OF THE FIRST STEP. "K" IS THE STEP COUN-
1300 C TER FOR THE EVALUATION OF THE DERIVATIVES; K=4 SIGNALS THAT FOUR
1400 C PASSES FOR THE CALCULATION OF DERIVATIVES ARE OVER FOR THE CUR-
1500 C RENT INTEGRATION STEP. SUBSCRIPTED VARIABLES ARE USED TO SAVE THE
1600 C AT THE I-TH STEP AND A,B,D,E ETC. ARE THE INCREMENT FUNCTION FOR
1700 C THE IMPROVED RUNGE FORMULAE
1800 C DIMENSION TGX(650),TWX(650),THX(650),TX2X(650)
1900 C DIMENSION C1X(650),C02NX(650),WX(650),WAX(650)
2000 C DIMENSION A(4),B(4),D(4),E(4)
2100 C OPEN (UNIT=1,DEVICE='DISK',FILE='LINE.FOR',ACCESS='SEQUENTIAL')
2200 C READ(1,61) L,CL,GR,GW,CPG,CPM
2300 C READ(1,61) TA,TGX(1),TWX(1),THX(1),TX2X(1)
2400 C READ(1,61) C1X(1),C02NX(1),WX(1),WAX(1)
2500 C READ(1,61) S,BX,Y1,Y2,Y3
2600 C READ(1,61) A1,A2,A3,A4,A5
2700 C CLOSE(UNIT=1,DEVICE='DISK',FILE='LINE.COR',DISPOSE='SAVE')
2800 C
2900 61 FORMAT (6F12.3)
3000 C HLOSS=0.0
3100 C HCALC=0.0
3200 C HVAR=0.0
3300 C *****
3400 C CALCULATION OF HEAT TRANSFER COEFFICIENTS
3500 C *****
3600 C J=CL
3700 C DO 20 I=1,L
3800 C IF(I-J) 11,11,8
3900 11 F1=10.02
4000 F2=97.21
4100 F3=44.13
4200 GO TO 9
4300 8 F1=5.01
4400 F2=4.02
4500 F3=39.12
4600 9 TG=TGX(I)
4700 TM=TWX(I)
4800 TW=TWX(I)
4900 TW2=TW2X(I)
5000 C1=C1X(I)
5100 W=WX(I)
5200 C02N=C02NX(I)
5300 WAX=WAX(I)
5400 DO 60 K=1,4
5500 10 H1=F1+(0.173E-8)*EG*EW*(TG**2+TW**2)*(TG+TW)
5600 H2=F2+(0.173E-8)*EG*EW*(TG**2+TM**2)*(TG+TM)
5700 H3=F3+(0.173E-8)*EW*EM*(A2/A3)*(TW**2+TM**2)*(TW+TM)
5800 H4=3.18
5900 H5=10.03
6000 Z1=H1*A1
6100 Z2=H2*A2
6200 Z3=H3*A3
6300 Z4=H4*A4
6400 Z5=H5*A5
6500 C *****
6600 C ITERATION FOR WALL TEMPERATURE
6700 C *****
6800 C Y1=((Z1+Z5)/(Z1+Z3+Z4)+Z4*Z5*TA)/(Z4+Z5)*(Z1+Z3+Z4)+74**2)
6900 C IF (ABS((Y1-TM)/TM).GE.0.01) GO TO 22
7000 C TW=Y1
7100 C GO TO 10
7200 22 TW2X(I)=(Z5*TA+Z4*TM)/(Z5+Z4)
7300 C TWX(I)=X1
7400 C AB=ABS(131377.0/TM)
7500 C IF (AB=0.0) 17,17,19
7600 17 R1=(1.393E27)*EXP(-131377.0/TM)
7700 C GO TO 111
7800 19 R1=0
7900 111 GS=GR*(1.0+0.786*C1+W)
8000 GG=GN*(1.0+WAX+C02N)
8100 C *****
8200 C RUNGE KUTTA CYCLE
8300 C *****
8400 C IF(672.0-TM)6,6,2
8500 2 RW=0
8600 C DTM=((Z2*(TG-TM)+Z3*(TM-TW)-Y1*BX*R1+C1-Y2*WX*RW)/(CP*GS)
8700 C GO TO 5
8800 6 IF(W=0.001) 2,2,13

```

```

9000 R0=(Z2*(TG-T1)+Z3*(T2-T1)-V1*BX*P1*(T1)/(Y2*BX)
9100 GU=10.5
9200 5 P1G=((Z2*BX*CF1*(U./86*F1+CF1+BW))*(T2-TG)+Z1*(TH-TG)-Y3)/(CPC+GG)
9300 PC1=((V1*U1+BX)/GD
9400 DA=((BX*BA)/G
9500 A(K)=U*DTG
9600 H(X)=S*DTG
9700 D(K)=S*DC1
9800 F(K)=S*DU
9900 IF(K=5)15,7,7
0000 15 TG=IGA(1)+0.5*B(K)
0100 TM=IMA(1)+0.5*A(K)
0200 C1=C1A(1)+0.5*D(K)
0300 W=W1(1)+0.5*E(K)
0400 GU=10.60
0500 7 TG=IGA(1)+B(K)
0600 TH=IMA(1)+A(K)
0700 C1=C1A(1)+D(K)
0800 W=W1(1)+E(K)
0900 60 CONTINUE
1000 C *****
1100 C IMPROVED FURTHER
1200 C *****
1300 TMX(I+1)=(TMX(I)+(A(1)+2.0*A(2)+2.0*A(3)+A(4))/6.0
1400 TGX(I+1)=TGX(1)+(B(1)+2.0*B(2)+2.0*B(3)+B(4))/6.0
1500 C1X(I+1)=C1A(1)+(U(1)+2.0*U(2)+2.0*U(3)+U(4))/6.0
1600 WX(I+1)=W1(1)+(E(1)+2.0*E(2)+2.0*E(3)+E(4))/6.0
1700 WNX(I+1)=(GB/GN)*(WX(I+1)-WX(1))+WNX(1)
1800 CU2NX(I+1)=(0.786*GB/GN)*(C1X(I+1)-C1X(1))+CU2NX(1)
1900 TA2X(I+1)=TA2X(1)
2000 TWX(I+1)=TWX(1)
2100 HLOSS=HLOSS+Z5*(TW2-TA)*S
2200 PRINT B4,I,TG,TH,W,C1,GS,GG,HVAF,HCALC,HLOSS
2300 64 FORMAT(5X,I3,2F7.0,2F7.2,5F11.3)
2400 20 CONTINUE
2500 STOP
2600 END

```

```

00100 C *****
00200 SIMULATION OF A ROTARY KILN FOR CEMENT
00300 C *****
00400 C THE FOLLOWING ALGORITHM FOR THE DIGITAL SIMULATION OF A CEMENT
00500 C ROTARY KILN EMPLOYS THE FOURTH ORDER "RUNGE-KUTTA METHOD" WITH
00600 C KUTIA'S COEFFICIENTS TO INTEGRATE A SYSTEM OF TEN SIMULTANEOUS
00700 C FIRST ORDER DIFFERENTIAL EQNS. FOR MASS & HEAT TRANSFER IN A
00800 C ROTARY KILN, ACROSS A STEP OF LENGTH "S" IN THE INDEPENDENT VAR-
00900 C IABLE "L", SUBJECT TO INITIAL CONDITIONS. EACH OF THE TEMPERATURE
01000 C & COMPOSITION DERIVATIVES MUST BE COMPUTED FOUR TIMES PER INTEG-
01100 C RATION STEP. "I" IS THE STEP COUNTER FOR EACH INTEGRATION STEP
01200 C AND EQUALS 1 AT THE END OF THE FIRST STEP. "K" IS THE STEP COUN-
01300 C TER FOR THE EVALUATION OF THE DERIVATIVES; K=4 SIGNALS THAT FOUR
01400 C PASSES FOR THE CALCULATION OF DERIVATIVES ARE OVER FOR THE CURRENT
01500 C INTEGRATION STEP. SUBSCRIPTED VARIABLES ARE USED TO SAVE THE VALUES
01600 C AT THE I-TH STEP AND A,B,C,D,E ETC. ARE THE INCREMENT FUNCTIONS FOR
01700 C THE IMPROVEMENT FORMULAE
01800 C *****
01900 DIMENSION TGX(950),TWX(950),TW2X(950),TMA(950)
02000 DIMENSION C1X(950),CO2NX(950),WX(950),WNX(950)
02100 DIMENSION YX(950),YX(950),CX(950),S1X(950)
02200 DIMENSION A(4),B(4),D(4),F(4),U(4),H(4),G(4)
02300 DIMENSION C1C(950),U(4)
02400 DIMENSION F(4)
02500 DS=894.0
02600 OPEN(UNIT=1,DEVICE='DSK',FILE='CEMENT .CDR',ACCESS='SEQUENTIAL')
02700 READ(1,61) L,IC,GB,ON,CPG,CPM
02800 READ(1,61) P,FG,EW
02900 READ(1,61) TA,TGX(1),TMA(1),TWX(1)
03000 READ(1,61) C1X(1),UA(1),CO2NX(1),WNA(1)
03100 READ(1,61) YX(1),YX(1),CX(1)
03200 READ(1,61) S1X(1),C1CX(1),S,RX
03300 READ(1,61) Y1,Y2,Y3,Y4,Y5
03400 READ(1,61) A1,A2,A3,A4,A5
03500 READ(1,62) U,H41,H42,KF
03600 FOR I=1/F12.3)
03700 FOR I=1/F12.3,E12.3,9X,13)
03800 FOR I=1/F12.4)
03900 CLOSE(UNIT=1,DEVICE='DSK',FILE='CEMENT.CDR',DISPOSE='SAVE')
04000 HCAT=0.0
04100 HVAL=0.0
04200 HLOSS=0.0
04300 C *****
04400 C CALCULATION OF HEAT TRANSFER COEFFICIENTS
04500 C *****
04600 J=IC
04700 DO 20 I=1,L
04800 IF(C1,11,0.001) FG=0.024
04900 IF(I-J) 11,11,8
05000 F1=10.02
05100 F2=97.21
05200 F3=44.13
05300 GU 10 9
05400 F1=5.01
05500 F2=4.02
05600 F3=39.12
05700 TG=TGX(I)
05800 TM=TMA(I)
05900 TW=TWX(I)
06000 TW2=TW2X(I)
06100 C1=C1X(I)
06200 W=WX(I)
06300 CO2W=CO2NX(I)
06400 WN=WNX(I)
06500 X=XX(I)
06600 Y=YX(I)
06700 C=CX(I)
06800 S1=S1X(I)
06900 C1C=C1CX(I)
07000 DO 60 K=1,4
07100 H1=F1+(0.173E-8)*EG*FW*(TG**2+TW**2)*(TG+TW)
07200 IF(1.GT.M) H1=0.0
07300 H2=F2+(0.173E-8)*EG*FM*(TG**2+TM**2)*(TG+TM)
07400 H3=F3+(0.173E-8)*EW*FM*(A2/A3)*(TW**2+TM**2)*(TW+TM)
07500 H4=H41
07600 IF(1.GT.M) H4=H42
07700 H5=10.03+(2.6678E-8)*(TW2**3+TA**3)
07800 DEL=(TW2-TA)
07900 Z1=H1*A1
08000 Z2=H2*A2
08100 Z3=H3*A3
08200 Z4=H4*A4
08300 Z5=H5*A5
08400 C *****
08500 C ITERATION FOR WALL TEMPERATURE
08600 C *****
08700 X1=((Z4+Z5)*((Z1*TG+Z3*TM)+Z4*Z5*TA)/((Z4+Z5)*(Z1+Z3+Z4)+Z5*Z5))
08800 IF(ABS(X1-1)/1W).LE.0.01) GO TO 22

```

```

8000 GU 10 10
9000 22 TW2A(1)=(Z5*TA+Z4*TL)/(Z5+Z4)
9100 TLX(1)=A1
9200 C
9300 AB=ABS(1313/7.0/TM)
9400 IF (AB-80.0) 17,11,19
9500 17 R1=(1.39327)*EXP(-131377.0/TM)
9600 GU 10 112
9700 19 R1=0
9800 112 CD=ABS(41592.3/10)
9900 IF (CD-80.0) 1,1,3
0000 GU 10 113
0100 3 R2=0
0200 113 EF=ABS(55458.47/TM)
0300 IF (EF-80.0) 23,23,24
0400 23 R3=(2.7868)*EXP(-EF)
0500 GU 10 111
0600 24 R3=0
0700 111 GS=GA*(1.0+0.786*(C1+C1C)+A)
0800 GG=GN*(1.0+AM+CU2H)
0900 C *****
1000 C RUNGE KUTIA CYCLE
1100 C *****
1200 IF (C1.GT.0.001) GU 10 37
1300 41 DIM=(Z2*(TG-TM)+Z3*(TW-TM))/(CPM*GS)
1400 IF (1.GT.4) DTG=-(TM-TA)/(1/Z3+1/Z4+1/Z5)*CPM*GS)
1500 42 DIC=(Z2*(TM-TG)+Z1*(TW-TG)-Y3)/(CPG*GG)
1600 IF (1.GT.4) DTG=(-EF)/(CPG*GG)
1700 GU 10 38
1800 37 IF (672.0-TM) 6,6,2
1900 2 RW=0
2000 DIM=(Z2*(TG-TM)+Z3*(TW-TM)-(D5*C1+1275.0*C1C)*BA*R1)/(CPM*GS)
2100 GU 10 5
2200 6 IF (K-0.001) 2,2,13
2300 13 DTM=0
2400 RW=(Z2*(TG-TM)+Z3*(TW-TM)-Y1*BX*R1*C1)/(Y2*BX)
2500 5 IF (C1.LT.0.001) C1=0.0
2600 IF (C1C.LT.0.001) C1C=0.0
2700 DIC=(Z2-BX*CPM*(0.786*R1*(C1+C1C)+RW))*(TM-TG)+Z1*(TW-TG)-Y3)/
2800 6 (CPG*GG)
2900 38 D1=-(K/BA)/GB
3000 D2=-D2*KX+SUR1(0)/GB
3100 D1=(1.0/143*R3*C*X*BX)/GB
3200
3300 DC1C=-R1*C1C*BX/GB
3400 DC1=-R1*C1*BX/GB
3500 DS1=-0.53571*R1*C1*BX/GB
3600 DX=-1.535/1*DC1-0.75439*DY
3700 DC=(D1*C1C-D2*C*X)*BX/GB
3800 IF (C1.GT.0.001) GU 10 33
3900 DC1=0
4000 DX=-0.75439*DY
4100 IF (C.LT.0.01) C=0.0
4200 DC=-(K3*C*X*BX)/GB
4300 33 IF (S1.GT.0.01) GU 10 34
4400
4500
4600 34 DS1=0
4700 IF (C1C.GT.0.001) GU 10 136
4800 136 A(K)=S*DTM
4900 B(K)=S*DTG
5000 D(K)=S*DC1
5100 E(K)=S*DW
5200 F(K)=S*DX
5300 G(K)=S*DY
5400 O(K)=S*DC
5500 H(K)=S*DS1
5600 U(K)=S*DC1C
5700 IF (K-3) 15,7,7
5800 15 TG=IGX(1)+0.5*B(K)
5900 TM=IMX(1)+0.5*A(K)
6000 C1=C1X(1)+0.5*D(K)
6100 W=WX(1)+0.5*E(K)
6200 X=XX(1)+0.5*F(K)
6300 Y=YX(1)+0.5*G(K)
6400 C=CX(1)+0.5*O(K)
6500 S1=S1X(1)+0.5*H(K)
6600 C1C=C1CX(1)+0.5*U(K)
6700 GU 10 60
6800 7 TG=IGX(1)+B(K)
6900 TM=IMX(1)+A(K)
7000 C1=C1X(1)+D(K)
7100 W=WX(1)+E(K)
7200 X=XX(1)+F(K)
7300 Y=YX(1)+G(K)
7400 C=CX(1)+O(K)
7500 S1=S1X(1)+H(K)
7600 C1C=C1CX(1)+U(K)

```

```

7800 C *****
7900 C IMPROVED F.F.T. FOURMULAE
8000 C *****
8100 TMX(T+1)=TMX(T)+(A(1)+2.0*A(2)+2.0*A(3)+A(4))/6.0
8200 TGX(T+1)=TGX(T)+(B(1)+2.0*B(2)+2.0*B(3)+B(4))/6.0
8300 C1X(T+1)=C1X(T)+(U(1)+2.0*U(2)+2.0*U(3)+U(4))/6.0
8400 WAX(T+1)=WAX(T)+(E(1)+2.0*E(2)+2.0*E(3)+E(4))/6.0
8500 WGX(T+1)=(GB/GU)*WAX(T+1)-WAX(T)+WAX(T)
8600 C02,X(T+1)=(0.786*GB/GU)*(C1X(T+1)+C1CX(T+1)-C1X(T)-C1CX(T))
8700 R+C02,X(T)
8800 T1,X(T+1)=1/WAX(T)
8900 T2,X(T+1)=T2,X(T)
9000 XA(T+1)=XA(T)+(F(1)+2.0*F(2)+2.0*F(3)+F(4))/6.0
9100 YA(T+1)=YA(T)+(G(1)+2.0*G(2)+2.0*G(3)+G(4))/6.0
9200 CX(T+1)=CX(T)+(O(1)+2.0*O(2)+2.0*O(3)+O(4))/6.0
9300 S1X(T+1)=S1X(T)+(H(1)+2.0*H(2)+2.0*H(3)+H(4))/6.0
9400 IF(J.GT.M) GO TO 72
9500
9600 HLOSS=HLOSS+Z5*(T2-TA)*S
9700 GU=1773
9800 HLOSS=HLOSS-0.01M*CPM*GS*S
72 73 C1CX(T+1)=C1CX(T)+(U(1)+2.0*U(2)+2.0*U(3)+U(4))/6.0
0000 IF(C1.LT.0.001) C1=0.0
0100 IF(C1C.LT.0.001) C1C=0.0
0200 HCALC=HCALC+GB*(DS*(C1X(T)-C1X(T+1))+(1*(C1CX(T)-C1CX(T+1)))
0300 HVAP=HVAP+GB*970.0*(WAX(T)-WAX(T+1))
0400 PRINT64,T,TG,T1,W,C1,C,X,Y,GS,GG,HVAP,HCALC,HLOSS
0500 64 F0PMAT(10A,13,2F7.0,5F7.2,5E11.3)
0600 20 CONTINUE
0700 STOP
0800 END

```

LIST OF CALCULATED VARIABLES

SYMBOL

DEFINITION

A	TOTAL TRANSFER AREA, SQ. FT./FT.
C	CLINKERABLE PORTLAND MASS, TONS/FT.
C ₁	CaO/UNIT CLINKERABLE MASS, LB./LB.
C ₂	CO ₂ AS CaCO ₃ /UNIT CLINKERABLE MASS, LB./LB.
C ₃	FREE CaO AS CaCO ₃ /UNIT CLINKERABLE MASS, LB./LB.
C ₄	CO ₂ /UNIT NITROGEN MASS, LB./LB.
C ₅	SPECIFIC HEAT OF GAS, BTU/LB. DEG. F
C ₆	SPECIFIC HEAT OF BURDEN MATERIAL, BTU/LB. DEG. F
C ₇	WISSIVITY OF GAS
C ₈	WISSIVITY OF BURDEN MATERIAL
C ₉	WISSIVITY OF WALL
C ₁₀	CO ₂ FLOW RATE, LB./HOUR
C ₁₁	GAS FLOW RATE, LB./HOUR
C ₁₂	THROUGH GAS FLOW RATE, LB./HOUR
C ₁₃	CO ₂ FLOW RATE, LB./HOUR
C ₁₄	WISS COEFFICIENT, HR. SQ. FT. DEG. F
C ₁₅	HEAT CONDUCTION FOR CALCINATION, BTU./HOUR
C ₁₆	HEAT CONDUCTION FOR EVAPORATION, BTU./HOUR
C ₁₇	HEAT LOSS THROUGH WALL, BTU./HOUR
C ₁₈	LOSS OF KILN, FT.
C ₁₉	KILN LENGTH, FT.
C ₂₀	TOTAL ACTIVE LENGTH OF KILN (without burning zone)
C ₂₁	RATE OF CALCINATION, PER HOUR
C ₂₂	RATE OF CLINKERING, PER HOUR
C ₂₃	RATE OF COMBUSTION/FT. OF BURNING ZONE
C ₂₄	RATE OF WATER EVAPORATION/UNIT CLINKERABLE MASS, LB.
C ₂₅	INTEGRATION STEP SIZE, FT.
C ₂₆	SiO ₂ /UNIT CLINKERABLE MASS, LB./LB.
C ₂₇	AMBIENT TEMPERATURE, DEG. RANKINE
C ₂₈	GAS TEMPERATURE, DEG. RANKINE
C ₂₉	MATERIAL TEMPERATURE, DEG. RANKINE
C ₃₀	INSIDE WALL TEMPERATURE, DEG. RANKINE
C ₃₁	WISS COEFFICIENT, DEG. RANKINE
C ₃₂	WISS COEFFICIENT, DEG. RANKINE
C ₃₃	WISS COEFFICIENT, DEG. RANKINE
C ₃₄	WISS COEFFICIENT, DEG. RANKINE
C ₃₅	WISS COEFFICIENT, DEG. RANKINE
C ₃₆	WISS COEFFICIENT, DEG. RANKINE
C ₃₇	WISS COEFFICIENT, DEG. RANKINE
C ₃₈	WISS COEFFICIENT, DEG. RANKINE
C ₃₉	WISS COEFFICIENT, DEG. RANKINE
C ₄₀	WISS COEFFICIENT, DEG. RANKINE
C ₄₁	WISS COEFFICIENT, DEG. RANKINE
C ₄₂	WISS COEFFICIENT, DEG. RANKINE
C ₄₃	WISS COEFFICIENT, DEG. RANKINE
C ₄₄	WISS COEFFICIENT, DEG. RANKINE
C ₄₅	WISS COEFFICIENT, DEG. RANKINE
C ₄₆	WISS COEFFICIENT, DEG. RANKINE
C ₄₇	WISS COEFFICIENT, DEG. RANKINE
C ₄₈	WISS COEFFICIENT, DEG. RANKINE
C ₄₉	WISS COEFFICIENT, DEG. RANKINE
C ₅₀	WISS COEFFICIENT, DEG. RANKINE
C ₅₁	WISS COEFFICIENT, DEG. RANKINE
C ₅₂	WISS COEFFICIENT, DEG. RANKINE
C ₅₃	WISS COEFFICIENT, DEG. RANKINE
C ₅₄	WISS COEFFICIENT, DEG. RANKINE
C ₅₅	WISS COEFFICIENT, DEG. RANKINE
C ₅₆	WISS COEFFICIENT, DEG. RANKINE
C ₅₇	WISS COEFFICIENT, DEG. RANKINE
C ₅₈	WISS COEFFICIENT, DEG. RANKINE
C ₅₉	WISS COEFFICIENT, DEG. RANKINE
C ₆₀	WISS COEFFICIENT, DEG. RANKINE
C ₆₁	WISS COEFFICIENT, DEG. RANKINE
C ₆₂	WISS COEFFICIENT, DEG. RANKINE
C ₆₃	WISS COEFFICIENT, DEG. RANKINE
C ₆₄	WISS COEFFICIENT, DEG. RANKINE
C ₆₅	WISS COEFFICIENT, DEG. RANKINE
C ₆₆	WISS COEFFICIENT, DEG. RANKINE
C ₆₇	WISS COEFFICIENT, DEG. RANKINE
C ₆₈	WISS COEFFICIENT, DEG. RANKINE
C ₆₉	WISS COEFFICIENT, DEG. RANKINE
C ₇₀	WISS COEFFICIENT, DEG. RANKINE
C ₇₁	WISS COEFFICIENT, DEG. RANKINE
C ₇₂	WISS COEFFICIENT, DEG. RANKINE
C ₇₃	WISS COEFFICIENT, DEG. RANKINE
C ₇₄	WISS COEFFICIENT, DEG. RANKINE
C ₇₅	WISS COEFFICIENT, DEG. RANKINE
C ₇₆	WISS COEFFICIENT, DEG. RANKINE
C ₇₇	WISS COEFFICIENT, DEG. RANKINE
C ₇₈	WISS COEFFICIENT, DEG. RANKINE
C ₇₉	WISS COEFFICIENT, DEG. RANKINE
C ₈₀	WISS COEFFICIENT, DEG. RANKINE
C ₈₁	WISS COEFFICIENT, DEG. RANKINE
C ₈₂	WISS COEFFICIENT, DEG. RANKINE
C ₈₃	WISS COEFFICIENT, DEG. RANKINE
C ₈₄	WISS COEFFICIENT, DEG. RANKINE
C ₈₅	WISS COEFFICIENT, DEG. RANKINE
C ₈₆	WISS COEFFICIENT, DEG. RANKINE
C ₈₇	WISS COEFFICIENT, DEG. RANKINE
C ₈₈	WISS COEFFICIENT, DEG. RANKINE
C ₈₉	WISS COEFFICIENT, DEG. RANKINE
C ₉₀	WISS COEFFICIENT, DEG. RANKINE
C ₉₁	WISS COEFFICIENT, DEG. RANKINE
C ₉₂	WISS COEFFICIENT, DEG. RANKINE
C ₉₃	WISS COEFFICIENT, DEG. RANKINE
C ₉₄	WISS COEFFICIENT, DEG. RANKINE
C ₉₅	WISS COEFFICIENT, DEG. RANKINE
C ₉₆	WISS COEFFICIENT, DEG. RANKINE
C ₉₇	WISS COEFFICIENT, DEG. RANKINE
C ₉₈	WISS COEFFICIENT, DEG. RANKINE
C ₉₉	WISS COEFFICIENT, DEG. RANKINE
C ₁₀₀	WISS COEFFICIENT, DEG. RANKINE

SUBSCRIPTS

1	GAS TO WALL
2	GAS TO SOLID
3	INSIDE WALL TO SOLID
4	INSIDE WALL TO OUTSIDE WALL
5	INSIDE WALL TO OUTSIDE WALL (in active zones)
6	INSIDE WALL TO OUTSIDE WALL (in burning zone)
7	OUTSIDE WALL TO AMBIENT

17	11	1	01	05	00	07AP	00ALC	00USS
836.	052.	2.10	0.87	0.143E+05	0.251E+05	0.000E+00	0.000E+00	0.000E+00
835.	054.	2.13	0.87	0.143E+05	0.251E+05	0.193E+05	0.000E+00	0.251E+05
832.	032.	2.12	0.87	0.142E+05	0.251E+05	0.139E+05	0.000E+00	0.528E+05
811.	032.	2.03	0.87	0.141E+05	0.249E+05	0.264E+05	0.000E+00	0.807E+05
810.	032.	2.05	0.87	0.139E+05	0.248E+05	0.393E+05	0.000E+00	0.109E+05
877.	031.	2.02	0.87	0.138E+05	0.247E+05	0.526E+05	0.000E+00	0.138E+05
831.	032.	1.94	0.87	0.137E+05	0.245E+05	0.664E+05	0.000E+00	0.167E+05
811.	032.	1.94	0.87	0.135E+05	0.244E+05	0.806E+05	0.000E+00	0.196E+05
819.	032.	1.93	0.87	0.134E+05	0.242E+05	0.952E+05	0.000E+00	0.226E+05
810.	032.	1.81	0.87	0.132E+05	0.241E+05	0.110E+07	0.000E+00	0.256E+05
809.	032.	1.81	0.87	0.130E+05	0.239E+05	0.125E+07	0.000E+00	0.286E+05
805.	032.	1.77	0.87	0.129E+05	0.238E+05	0.141E+07	0.000E+00	0.317E+05
870.	032.	1.73	0.87	0.127E+05	0.236E+05	0.157E+07	0.000E+00	0.347E+05
870.	032.	1.68	0.87	0.126E+05	0.235E+05	0.173E+07	0.000E+00	0.378E+05
870.	032.	1.54	0.87	0.124E+05	0.233E+05	0.189E+07	0.000E+00	0.410E+05
861.	032.	1.53	0.87	0.122E+05	0.231E+05	0.206E+07	0.000E+00	0.441E+05
863.	032.	1.51	0.87	0.120E+05	0.230E+05	0.223E+07	0.000E+00	0.473E+05
851.	032.	1.50	0.87	0.119E+05	0.228E+05	0.240E+07	0.000E+00	0.505E+05
845.	032.	1.45	0.87	0.117E+05	0.226E+05	0.258E+07	0.000E+00	0.537E+05
839.	032.	1.40	0.87	0.115E+05	0.224E+05	0.275E+07	0.000E+00	0.570E+05
1000.	032.	1.35	0.87	0.113E+05	0.222E+05	0.293E+07	0.000E+00	0.602E+05
1005.	032.	1.30	0.87	0.111E+05	0.221E+05	0.311E+07	0.000E+00	0.635E+05
1007.	032.	1.25	0.87	0.109E+05	0.219E+05	0.329E+07	0.000E+00	0.668E+05
1010.	032.	1.20	0.87	0.108E+05	0.217E+05	0.347E+07	0.000E+00	0.701E+05
1012.	032.	1.15	0.87	0.106E+05	0.215E+05	0.366E+07	0.000E+00	0.734E+05
1015.	032.	1.10	0.87	0.104E+05	0.213E+05	0.384E+07	0.000E+00	0.767E+05
1017.	032.	1.05	0.87	0.102E+05	0.211E+05	0.403E+07	0.000E+00	0.800E+05
1019.	032.	1.00	0.87	0.999E+04	0.209E+05	0.422E+07	0.000E+00	0.834E+05
1021.	032.	0.94	0.87	0.980E+04	0.207E+05	0.441E+07	0.000E+00	0.867E+05
1023.	032.	0.89	0.87	0.960E+04	0.205E+05	0.460E+07	0.000E+00	0.901E+05
1025.	032.	0.84	0.87	0.940E+04	0.203E+05	0.479E+07	0.000E+00	0.935E+05
1026.	032.	0.78	0.87	0.920E+04	0.201E+05	0.498E+07	0.000E+00	0.969E+05
1028.	032.	0.73	0.87	0.900E+04	0.199E+05	0.518E+07	0.000E+00	0.100E+06
1029.	032.	0.68	0.87	0.880E+04	0.197E+05	0.537E+07	0.000E+00	0.104E+06
1030.	032.	0.62	0.87	0.860E+04	0.195E+05	0.557E+07	0.000E+00	0.107E+06
1031.	032.	0.57	0.87	0.840E+04	0.193E+05	0.576E+07	0.000E+00	0.110E+06
1033.	032.	0.52	0.87	0.820E+04	0.191E+05	0.596E+07	0.000E+00	0.114E+06
1035.	032.	0.46	0.87	0.800E+04	0.189E+05	0.616E+07	0.000E+00	0.117E+06
1035.	032.	0.41	0.87	0.780E+04	0.187E+05	0.635E+07	0.000E+00	0.121E+06
1036.	032.	0.35	0.87	0.760E+04	0.185E+05	0.655E+07	0.000E+00	0.124E+06
1037.	032.	0.30	0.87	0.738E+04	0.183E+05	0.675E+07	0.000E+00	0.128E+06
1038.	032.	0.24	0.87	0.718E+04	0.181E+05	0.695E+07	0.000E+00	0.131E+06
1038.	032.	0.19	0.87	0.697E+04	0.179E+05	0.715E+07	0.000E+00	0.135E+06
1030.	032.	0.13	0.87	0.676E+04	0.177E+05	0.735E+07	0.000E+00	0.138E+06
1040.	032.	0.08	0.87	0.656E+04	0.175E+05	0.755E+07	0.000E+00	0.141E+06
1040.	032.	0.02	0.87	0.635E+04	0.173E+05	0.775E+07	0.000E+00	0.145E+06
1037.	032.	0.02	0.87	0.618E+04	0.171E+05	0.794E+07	0.000E+00	0.148E+06
1053.	030.	-0.00	0.87	0.626E+04	0.170E+05	0.784E+07	0.000E+00	0.152E+06
1066.	030.	-0.00	0.87	0.626E+04	0.170E+05	0.784E+07	0.000E+00	0.156E+06
1093.	032.	-0.00	0.87	0.626E+04	0.170E+05	0.784E+07	0.000E+00	0.162E+06
1123.	035.	-0.00	0.87	0.626E+04	0.170E+05	0.784E+07	0.000E+00	0.167E+06
1152.	032.	-0.00	0.87	0.626E+04	0.170E+05	0.784E+07	0.000E+00	0.172E+06
1161.	035.	-0.00	0.87	0.626E+04	0.170E+05	0.784E+07	0.000E+00	0.178E+06
1210.	030.	-0.00	0.87	0.626E+04	0.170E+05	0.784E+07	0.000E+00	0.183E+06
1239.	030.	-0.00	0.87	0.626E+04	0.170E+05	0.784E+07	0.000E+00	0.190E+06
1265.	1020.	-0.00	0.87	0.626E+04	0.170E+05	0.784E+07	0.000E+00	0.196E+06
1293.	1042.	-0.00	0.87	0.626E+04	0.170E+05	0.784E+07	0.000E+00	0.203E+06
1320.	1066.	-0.00	0.87	0.626E+04	0.170E+05	0.784E+07	0.000E+00	0.210E+06
1346.	1090.	-0.00	0.87	0.626E+04	0.170E+05	0.784E+07	0.000E+00	0.217E+06
1373.	1115.	-0.00	0.87	0.626E+04	0.170E+05	0.784E+07	0.000E+00	0.225E+06
1399.	1140.	-0.00	0.87	0.626E+04	0.170E+05	0.784E+07	0.000E+00	0.233E+06
1425.	1167.	-0.00	0.87	0.626E+04	0.170E+05	0.784E+07	0.000E+00	0.241E+06
1451.	1193.	-0.00	0.87	0.626E+04	0.170E+05	0.784E+07	0.000E+00	0.250E+06
1476.	1221.	-0.00	0.87	0.626E+04	0.170E+05	0.784E+07	0.000E+00	0.259E+06
1501.	1250.	-0.00	0.87	0.626E+04	0.170E+05	0.784E+07	0.000E+00	0.268E+06
1527.	1278.	-0.00	0.87	0.626E+04	0.170E+05	0.784E+07	0.000E+00	0.278E+06
1552.	1306.	-0.00	0.87	0.626E+04	0.170E+05	0.784E+07	0.000E+00	0.288E+06
1577.	1334.	-0.00	0.87	0.626E+04	0.170E+05	0.784E+07	0.000E+00	0.298E+06
1600.	1362.	-0.00	0.87	0.626E+04	0.170E+05	0.784E+07	0.000E+00	0.309E+06
1625.	1390.	-0.00	0.87	0.626E+04	0.170E+05	0.784E+07	0.000E+00	0.319E+06
1649.	1417.	-0.00	0.87	0.626E+04	0.170E+05	0.784E+07	0.000E+00	0.331E+06
1673.	1445.	-0.00	0.87	0.626E+04	0.170E+05	0.784E+07	0.000E+00	0.342E+06
1697.	1472.	-0.00	0.87	0.626E+04	0.170E+05	0.784E+07	0.000E+00	0.354E+06
1721.	1500.	-0.00	0.87	0.626E+04	0.170E+05	0.784E+07	0.000E+00	0.366E+06
1744.	1528.	-0.00	0.87	0.626E+04	0.170E+05	0.784E+07	0.000E+00	0.379E+06
1768.	1556.	-0.00	0.87	0.626E+04	0.170E+05	0.784E+07	0.000E+00	0.392E+06
1791.	1584.	-0.00	0.87	0.626E+04	0.170E+05	0.784E+07	0.000E+00	0.405E+06
1814.	1612.	-0.00	0.87	0.626E+04	0.170E+05	0.784E+07	0.000E+00	0.418E+06
1838.	1640.	-0.00	0.87	0.626E+04	0.170E+05	0.784E+07	0.000E+00	0.431E+06
1861.	1668.	-0.00	0.87	0.626E+04	0.170E+05	0.784E+07	0.000E+00	0.444E+06

[illegible]

4 2	2 6	2 11	2 20	2 34F+0.4	0.151E+0.5	0.104E+0.1	0.214E+0.7	0.211E+0.7
4 2	2 3	2 10	2 17	2 32F+0.4	0.151E+0.5	0.104E+0.1	0.322E+0.7	0.213E+0.7
4 3	2 7	2 12	2 15	2 32F+0.4	0.150E+0.5	0.104E+0.1	0.332E+0.7	0.216E+0.7
4 3	2 6	2 10	2 13	0.149E+0.5	0.149E+0.5	0.104E+0.1	0.341E+0.7	0.218E+0.7
4 3	2 7	2 12	2 13	0.149E+0.5	0.149E+0.5	0.104E+0.1	0.350E+0.7	0.220E+0.7
4 3	2 7	2 12	2 16	0.148E+0.5	0.148E+0.5	0.104E+0.1	0.359E+0.7	0.222E+0.7
4 3	2 5	2 10	2 17	0.148E+0.5	0.148E+0.5	0.104E+0.1	0.369E+0.7	0.224E+0.7
4 4	2 2	2 9	2 15	0.147E+0.5	0.147E+0.5	0.104E+0.1	0.378E+0.7	0.226E+0.7
4 4	2 3	2 10	2 16	0.146E+0.5	0.146E+0.5	0.104E+0.1	0.387E+0.7	0.228E+0.7
4 4	2 5	2 12	2 17	0.146E+0.5	0.146E+0.5	0.104E+0.1	0.396E+0.7	0.230E+0.7
4 4	2 6	2 12	2 17	0.145E+0.5	0.145E+0.5	0.104E+0.1	0.405E+0.7	0.233E+0.7
4 5	2 2	2 9	2 16	0.145E+0.5	0.145E+0.5	0.104E+0.1	0.412E+0.7	0.235E+0.7
4 5	2 11	2 20	2 22	0.145E+0.5	0.145E+0.5	0.104E+0.1		

[illegible]

[illegible]

[illegible]

1947	1948	1949	1950	1951	1952	1953	1954	1955	1956	1957	1958	1959	1960	1961	1962	1963	1964	1965	1966	1967	1968	1969	1970	1971	1972	1973	1974	1975	1976	1977	1978	1979	1980	1981	1982	1983	1984	1985	1986	1987	1988	1989	1990	1991	1992	1993	1994	1995	1996	1997	1998	1999	2000	2001	2002	2003	2004	2005	2006	2007	2008	2009	2010	2011	2012	2013	2014	2015	2016	2017	2018	2019	2020	2021	2022	2023	2024	2025	2026	2027	2028	2029	2030	2031	2032	2033	2034	2035	2036	2037	2038	2039	2040	2041	2042	2043	2044	2045	2046	2047	2048	2049	2050	2051	2052	2053	2054	2055	2056	2057	2058	2059	2060	2061	2062	2063	2064	2065	2066	2067	2068	2069	2070	2071	2072	2073	2074	2075	2076	2077	2078	2079	2080	2081	2082	2083	2084	2085	2086	2087	2088	2089	2090	2091	2092	2093	2094	2095	2096	2097	2098	2099	2100	2101	2102	2103	2104	2105	2106	2107	2108	2109	2110	2111	2112	2113	2114	2115	2116	2117	2118	2119	2120	2121	2122	2123	2124	2125	2126	2127	2128	2129	2130	2131	2132	2133	2134	2135	2136	2137	2138	2139	2140	2141	2142	2143	2144	2145	2146	2147	2148	2149	2150	2151	2152	2153	2154	2155	2156	2157	2158	2159	2160	2161	2162	2163	2164	2165	2166	2167	2168	2169	2170	2171	2172	2173	2174	2175	2176	2177	2178	2179	2180	2181	2182	2183	2184	2185	2186	2187	2188	2189	2190	2191	2192	2193	2194	2195	2196	2197	2198	2199	2200	2201	2202	2203	2204	2205	2206	2207	2208	2209	2210	2211	2212	2213	2214	2215	2216	2217	2218	2219	2220	2221	2222	2223	2224	2225	2226	2227	2228	2229	2230	2231	2232	2233	2234	2235	2236	2237	2238	2239	2240	2241	2242	2243	2244	2245	2246	2247	2248	2249	2250	2251	2252	2253	2254	2255	2256	2257	2258	2259	2260	2261	2262	2263	2264	2265	2266	2267	2268	2269	2270	2271	2272	2273	2274	2275	2276	2277	2278	2279	2280	2281	2282	2283	2284	2285	2286	2287	2288	2289	2290	2291	2292	2293	2294	2295	2296	2297	2298	2299	2300	2301	2302	2303	2304	2305	2306	2307	2308	2309	2310	2311	2312	2313	2314	2315	2316	2317	2318	2319	2320	2321	2322	2323	2324	2325	2326	2327	2328	2329	2330	2331	2332	2333	2334	2335	2336	2337	2338	2339	2340	2341	2342	2343	2344	2345	2346	2347	2348	2349	2350	2351	2352	2353	2354	2355	2356	2357	2358	2359	2360	2361	2362	2363	2364	2365	2366	2367	2368	2369	2370	2371	2372	2373	2374	2375	2376	2377	2378	2379	2380	2381	2382	2383	2384	2385	2386	2387	2388	2389	2390	2391	2392	2393	2394	2395	2396	2397	2398	2399	2400
------	------	------	------	------	------	------	------	------	------	------	------	------	------	------	------	------	------	------	------	------	------	------	------	------	------	------	------	------	------	------	------	------	------	------	------	------	------	------	------	------	------	------	------	------	------	------	------	------	------	------	------	------	------	------	------	------	------	------	------	------	------	------	------	------	------	------	------	------	------	------	------	------	------	------	------	------	------	------	------	------	------	------	------	------	------	------	------	------	------	------	------	------	------	------	------	------	------	------	------	------	------	------	------	------	------	------	------	------	------	------	------	------	------	------	------	------	------	------	------	------	------	------	------	------	------	------	------	------	------	------	------	------	------	------	------	------	------	------	------	------	------	------	------	------	------	------	------	------	------	------	------	------	------	------	------	------	------	------	------	------	------	------	------	------	------	------	------	------	------	------	------	------	------	------	------	------	------	------	------	------	------	------	------	------	------	------	------	------	------	------	------	------	------	------	------	------	------	------	------	------	------	------	------	------	------	------	------	------	------	------	------	------	------	------	------	------	------	------	------	------	------	------	------	------	------	------	------	------	------	------	------	------	------	------	------	------	------	------	------	------	------	------	------	------	------	------	------	------	------	------	------	------	------	------	------	------	------	------	------	------	------	------	------	------	------	------	------	------	------	------	------	------	------	------	------	------	------	------	------	------	------	------	------	------	------	------	------	------	------	------	------	------	------	------	------	------	------	------	------	------	------	------	------	------	------	------	------	------	------	------	------	------	------	------	------	------	------	------	------	------	------	------	------	------	------	------	------	------	------	------	------	------	------	------	------	------	------	------	------	------	------	------	------	------	------	------	------	------	------	------	------	------	------	------	------	------	------	------	------	------	------	------	------	------	------	------	------	------	------	------	------	------	------	------	------	------	------	------	------	------	------	------	------	------	------	------	------	------	------	------	------	------	------	------	------	------	------	------	------	------	------	------	------	------	------	------	------	------	------	------	------	------	------	------	------	------	------	------	------	------	------	------	------	------	------	------	------	------	------	------	------	------	------	------	------	------	------	------	------	------	------	------	------	------	------	------	------	------	------	------	------	------	------